Published in Physical Properties and Thermodynamic Behaviour of Minerals, NATO ASI Series C, Vol. 225, edited by E.K.H. Salje, D. Reidel Publishing Company (1988).

EXSOLUTION, ORDERING AND STRUCTURAL TRANSFORMATIONS: SYSTEMATICS AND SYNERGISTICS

D. E. Laughlin
Dept. of Metallurgical Engineering & Materials Science
Carnegie Mellon University
Pittsburgh, PA 15213 USA

W. A. Soffa
Dept. of Materials Science and Engineering
University of Pittsburgh
Pittsburgh, PA 15261 USA

ABSTRACT. Various paths of transformation can occur in metallic and non-metallic solid solutions depending on the thermodynamic stability of the initial state with respect to the relevant order parameters describing composition, atomic ordering, magnetic ordering, strain, *etc.* The particular reaction path followed by the system can have a profound influence on the resultant microstructure and properties of the material. Of particular importance in real systems is often the influence of the different possible ordering tendencies on the phase diagram and their complex interplay during transformation. In this paper reactions such as exsolution or phase separation, atomic ordering, magnetic ordering, *etc.* will be discussed with emphasis on the interaction of higher order transitions with first order phase boundaries in the phase diagram and on the synergistics of different ordering tendencies during transformation. Extensive use of free energy diagrams is employed as a tool to systematize the phase equilibria and the various multistage reaction paths accessible to the system.

1. INTRODUCTION

A single phase solid solution, α, which is stable when it has a particular set of intensive thermodynamic parameters, T,P,... may become metastable or unstable with respect to the formation of another phase, β, when one or more of these parameters are altered. The reaction which ensues may be termed exsolution, precipitation or decomposition.* A description of the paths that

*In the metallurgical literature decomposition is used in a synonymous fashion to "exsolution". Many metallic alloys when they undergo exsolution form solid solutions that are based on their elemental constituents. Hence the term "decomposition" is appropriate.

such a solid solution passes through in order to attain thermodynamic equilibrium involves a knowledge of the phase diagram, the symmetry of the phases α and β, interphase interfacial free energies, as well as kinetic parameters such as diffusivity, *etc.* In this article we discuss several types of exsolution reactions that commonly occur in metallic or nonmetallic solid solutions.

We begin with the simplest exsolution reaction, namely one in which both the α and β phases have the same crystal structure, differing only in their respective compositions (**2.1**). This *isostructural* reaction can be modeled by only one "order parameter", namely the difference in composition between the two ensuing phases. The equilibrium value of this order parameter changes discontinuously at all points along the phase boundary (except at the critical point) and hence these transformations are thermodynamically classified as *first order.* We consider such exsolution reactions at both small supersaturations (**2.2**) and large supersaturations (**2.3**), namely under conditions in which the reaction may be modeled as nucleation or spinodal decomposition, respectively. We also discuss the case in which the supersaturation is of intermediate value, *viz.* the reaction occurs near the spinodal. In the discussion of spinodal decomposition, we differentiate between the microstructure of the reaction occurring in isotropic elastic media and that occurring in an anisotropic (cubic) elastic medium.

Another simple solid state reaction occurs when the parent α phase transforms entirely into an atomically ordered phase β, which is a crystallographic derivative (Buerger, 1947) of the α phase (**3.1**). In this case the reaction can be described by the long range (atomic) order parameter η. Such ordering reactions may be thermodynamically of either *first order* (**3.2.2**) or *higher order*** (**3.2.1**).

When a line of higher order transitions ends on a first order phase boundary, a *critical end* point exists (Allen and Cahn, 1982). If such a line terminates uniquely at the critical point of a two phase region, a *tricritical* point is produced at which three phases become indistinguishable (Griffiths, 1970 and 1974). Phase diagrams exhibiting *tricritical points* are herein presented, and the various possible reaction paths that exist for solid solutions exhibiting *tricritical* behavior are discussed (**3.2.1**).

The final sections (**4** and **5**) introduce another ordering reaction, namely "magnetic ordering". This entails an additional order parameter (**M**,

---

**We prefer to use the term "higher order" because of the difficulty in distinguishing between "second", "third", etc. order transitions. All "higher order" transitions are continuous at the transition temperature.

magnetization, for the ferromagnetic case). This ordering process interacts with first order phase boundaries in a similar fashion as does the higher order atomic order/disorder reactions. Examples of such phase diagrams are discussed (4). Finally, phase diagrams exhibiting atomic and magnetic ordering are discussed. Here, the *bicritical* and tetracritical points are introduced, (5) and the salient features of such reactions discussed.

The emphasis of the paper is to discuss how various ordering reactions in solid solutions interact with each other. Of particular concern is how their interaction affects phase equilibria, phase diagrams, free energy curves, as well as how their interaction affects the paths through which the solid solution passes in attaining thermodynamic equilibrium (metastable or stable). Although the diagrams used in the paper are schematic, many are idealizations of actual phase diagrams that describe minerals and/or metallic alloys. Of course many equilibrium phase diagrams are much more complicated than those discussed herein. In these diagrams, the conjugate phases may not be crystallographic derivatives of the high temperature disordered phase. Nevertheless, *metastable* phase equilibria may obtain in these systems because of kinetic considerations. Only after extended times will the equilibrium phases appear. In such cases, the *metastable equilibria* and corresponding *metastable* transition sequence may be modeled as done herein. Indeed, in metallurgical systems, many of the phase transitions that give rise to important changes in mechanical and physical properties (mechanical strengthening, magnetic hardening, *etc.*) are metastable ones, the equilibrium phases or structures often being undesirable.

2. ISOSTRUCTURAL DECOMPOSITION

2.1. Introduction

We begin our discussion of isostructural decomposition by considering the phase diagram shown in Figure 1. An alloy of composition C_0 is in a single phase region of the diagram at T_0 and within a two phase region at temperature T_A. From the point of view of *configurational entropy*, the high temperature state is *disordered*, while the equilibrium low temperature state consisting of two phases is *ordered*. The two phases differ from one another only in their composition; they have identical crystal structures (*isostructural decomposition*). Thus, in following the decomposition of the high temperature phase the relevant order parameter is the difference in composition, ΔC, between the various regions within the material.

Two distinct decomposition behaviours can be observed for a

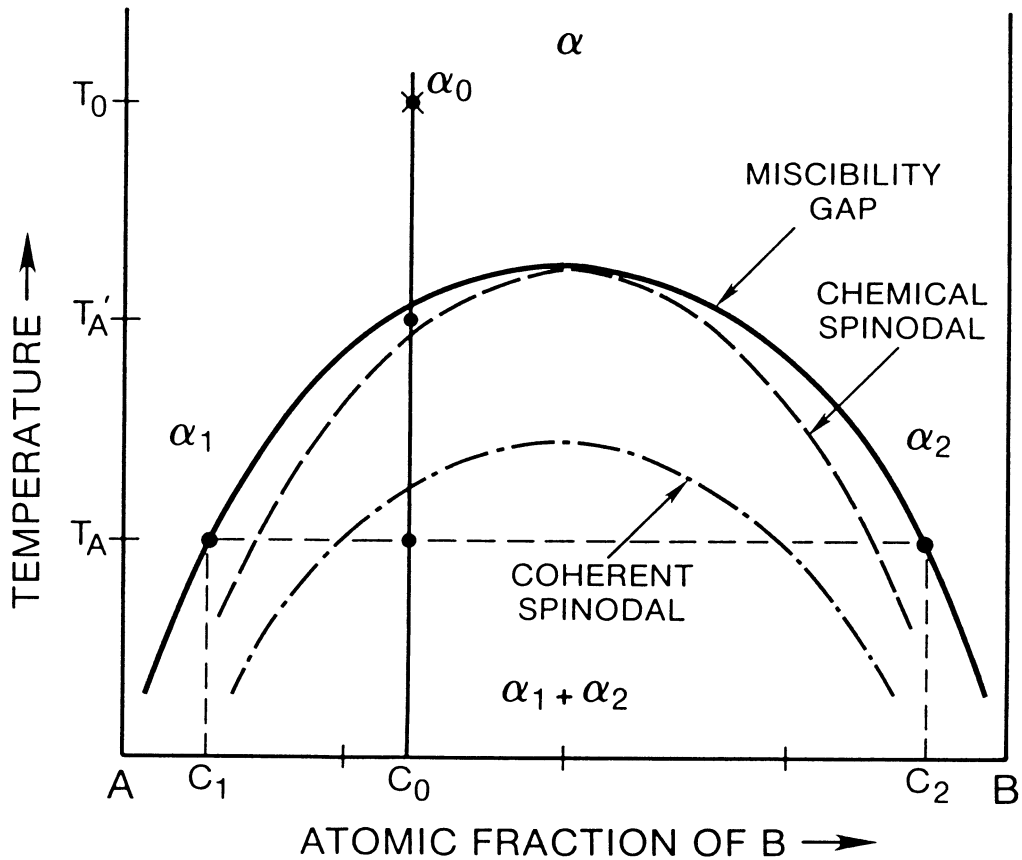

Figure 1. Schematic phase diagram of a binary solution exhibiting a miscibility gap in the solid state. Both the chemical and coherent spinodal lines are depicted.

supersaturated solid solution of an alloy that is quenched from the single phase region into the two phase region. For shallow quenches (small supersaturations) the initiation of decomposition derives from fluctuations in which the order parameter, ΔC, undergoes relatively large changes within regions of small spatial extent. In such a process the embryos or "nuclei" of the new phase are formed randomly within the matrix. This is the decomposition path that has been described by the classical nucleation and growth models (Christian, 1975). At large undercoolings, the alloy decomposes along paths in which the change of the order parameter, ΔC, is initially small, but the extent over which it changes is large. Such a process involving the progressive development of initially low amplitude, highly extended fluctuations has been termed *spinodal decomposition* (Cahn, 1961, 1962a). (For reviews on spinodal decomposition see Cahn, 1968; Hilliard, 1970; and de Fontaine, 1970.)

Classical nucleation and spinodal decomposition represent extremes in a decomposition spectrum characterized by a gradual transition from metastability to instability. The Cahn-Hilliard nonclassical homogeneous nucleation theory (Cahn and Hilliard, 1958; 1959) essentially provides the critical linkage for understanding the progressive change in the nature of the behavior of the decomposition process as the supersaturation or undercooling is increased. As the supersaturation is increased the critical nucleus rapidly becomes diffuse and progressively exhibits characteristics which are very different from those of the "classical nucleus". The amplitude of the critical fluctuation deviates from the equilibrium composition and the interface between the incipient precipitate and parent phase becomes markedly extended. Furthermore, as the spinodal is approached the "nucleation barrier" approaches kT, and a range of finite-amplitude fluctuations against which the system is unstable becomes part of the spectrum of frequently occurring fluctuations. Hence the concept of a well-defined critical nucleus loses its meaning. A variety of fluctuations of varying spatial extent and amplitude readily leads to decomposition of the supersaturated state. This transition regime extends both above and below the spinodal. Thus, the transition from metastability to instability is characterized by a process in which the reaction path does not necessarily minimize the free energy of formation of the critical fluctuation but rather maximizes the rate of decomposition (Cahn, 1962b; Langer, 1975; Aaronson and Russell, 1982). Although it has been repeatedly pointed out (Hillert, 1956; de Fontaine, 1969; Martin, 1979) that the boundary between the extreme behavior is not sharp, it has been the practice of experimentalists to attempt to denote the temperature at which the behaviour changes.

2.2 Nucleation and Growth

Let us first look at the nucleation behaviour for coherent *isostructural* exsolution in a *cubic* system. The free energy change accompanying the formation of an embryo of the new phase may be written as:

$$\Delta G = (g_v + E_s)V + \sigma A$$

where g_v is the bulk chemical free energy per unit volume of the new phase

E_s is the strain energy per unit volume produced by the new phase

σ is the surface energy of the interphase interphase between the new phase and the matrix

V is the volume and A the surface area of the new phase

The equation shows that thermodynamically the optimum shape of the new phase generally will represent a compromise between the surface and strain energies. For the case of small atomic misfit or mismatch the particle of the new phase is expected to be a sphere if σ is isotropic. As the particle grows the strain energy becomes more important, and may cause the sphere to change its shape. The elastic anisotropy of the cubic matrix may result in facets normal to the elastically "soft" directions, (e.g. <100>) producing cuboids. However, if σ is anisotropic, initially the new phase would take a shape dictated by the surface energy anisotropy, *viz.* facets would be present on the "critical nuclei". The symmetry of the shape of the particle of the new phase would include the symmetry of the point group of its crystal structure, *viz.*, it would be at least $m\bar{3}m$. If, for example, the {111} planes minimize σ, an octahedral particle would be favored. If the {100} planes, on the other hand, represent a minimum for σ, a cuboid would form. Finally, if the {100} and {111} planes are of similar magnitude, a tetrakaidecahedral (14 sided) particle would form. As the particle grows, the strain energy which scales with the volume begins to impose shape effects which eventually may dominate the morphology.

For large atomic misfit, the shape of the particle of the new phase would be dominated by strain energy considerations from the start of its existence. This often gives rise to plate like precipitates of the new phase. The normals to the plates lie along the elastically soft directions of the matrix. Examples

of isostructural decomposition with large misfit in metallic alloys include the so-called Guinier-Preston zones in Al-Cu and Cu-Be. As the volume fraction of the second phase increases (either with time at temperature or with increasing supersaturation) the strain fields of the precipitates begin to interact. This may lead to particle alignment along the elastically soft directions and even to the development of spatially correlated precipitates (Tiapkin, 1977).

2.3 Spinodal Decomposition

At large supersaturations, the decomposition process proceeds in a manner which has been termed *spinodal* decomposition. As discussed above, the spinodal reaction is a spontaneous unmixing or diffusional clustering whose behaviour is distinct from classical nucleation and growth in metastable solutions. This different kinetic behavior, which does not require a nucleation step, was first described by J.W. Gibbs in his treatment of the thermodynamic stability of undercooled or supersaturated phases. The *spinodal* line in Figure 1 indicates an instability with respect to the response of the system to compositional fluctuations. The locus, called the "chemical spinodal", is defined by the inflexion points of the isothermal free energy (G) composition curves ($\partial^2 G/\partial C^2 = G'' = 0$). Within the spinodes where $G'' < 0$, the supersaturated solution is unstable with respect to unmixing and spinodal decomposition can occur. It should be remembered, as discussed above, that this stability limit is by no means sharp; rather a region exists in which the metastable solution gradually begins to display nonclassical decomposition behavior. Spinodal decomposition or continuous phase separation essentially involves the selective amplification of long wavelength concentration waves within the supersaturated state resulting from uphill diffusion as a consequence of the inherent thermodynamic instability of the system. The transformation occurs homogeneously throughout the alloy *via* the gradual buildup of regions alternatively enriched or depleted in solute, resulting in a two-phase modulated structure.

The essential features of the spinodal process can be understood by considering this diffusional clustering as the inverse of the homogenization of a nonuniform solid solution exhibiting a sinusoidal variation of composition with distance. (A sinusoidal composition wave is rather general, because it may be viewed as a Fourier component of an arbitrary composition variation.) In metastable solutions the small deviations from the average concentration, C_0, will decay with time according to the equation

$$\Delta C = \Delta C_0 \exp(-t/\tau)$$

where ΔC_0 is the amplitude, the relaxation time $\tau \sim \lambda^2/\tilde{D}$; λ is the wavelength

of the fluctuation or Fourier component and $\tilde{D}$ is the appropriate diffusion coefficient. In a binary system $\tilde{D} \propto G''$, and within the spinodes $G'' < 0$; that is, the curvature of the free energy *versus* composition curve is negative. Therefore, in an unstable solid solution $\tilde{D}$ is negative, and "uphill" diffusion occurs, resulting in spontaneous unmixing. The amplitude of the concentration wave grows with time, that is, $\Delta C = \Delta C_0 \exp(+R(\beta)t)$, where the amplification factor $R(\beta)$ is a function of the wave number $\beta = 2\pi/\lambda$. The factor $R(\beta)$ is a maximum for intermediate wavelengths. Long wavelength fluctuations grow sluggishly because of the large diffusion distances; short wavelength fluctuations are suppressed by the so-called gradient or surface energy of the diffuse or incipient interfaces that evolve during phase separation. Therefore, the microstructure that develops during spinodal decomposition has a characteristic periodicity that is typically 2.5 to 10 nm (25 to 100 Å) in metallic systems.

The factors controlling the spinodal reaction and resultant structures are clarified by examining the energetics of small-amplitude composition fluctuations in solid solutions. The free energy of an inhomogeneous solution expressed as an integral over the volume, V, of the crystal can be written as:

$$G = \int \left\{ f(C) + K\nabla C^2 + E_s \right\} dV$$

where f(C) is the free energy per unit volume of a uniform solution of composition C, K is the gradient energy parameter, and E_s is a strain energy term that depends on the elastic constants and misfit (difference in lattice parameter) between the solute-enriched and solute-depleted regions. For a sinusoidal composition fluctuation

$$C - C_0 = A \sin \beta x$$

(where A is the amplitude of the sine wave), the gradient or surface energy term varies as $K\beta^2$ and prohibits decomposition on too fine a scale. The wavelength of the dominant concentration wave that essentially determines the scale of decomposition varies as $K^{1/2}(\Delta T)^{-1/2}$, where $\Delta T = T_s - T_A$, in which T_s is the *spinodal temperature* and T_A is the reaction temperature. The coherency strain energy term is independent of wavelength, but can vary markedly with crystallographic direction in elastically anisotropic crystals. Therefore, the dominant concentration waves will develop along elastically "soft" directions in anisotropic systems. For most cubic materials, the <100> directions are preferred, although <111> waves are predicted in certain alloys, depending on the so-called anisotropy factor. The strain energy can also stabilize the system against exsolution and effectively displace the spinodal curve (and the solvus), thus defining a "coherent spinodal" (Cahn, 1962a; See Figure 1).

Periodic composition fluctuations in the decomposing solid solution cause diffraction effects known as "satellites" or "sidebands". The fundamental reflections in reciprocal space are flanked by satellites or secondary maxima, and the distance of the satellites from the fundamental varies inversely with the wavelength of the growing concentration wave. This diffuse scattering arises from the periodic variation of the lattice parameter and/or scattering factor. The strain effects are negligible around the origin of reciprocal space. Thus, small-angle x-ray and neutron scattering can be used to study quantitatively the kinetics of the reaction by monitoring the changes in the intensity distribution around the direct beam due to changes in the structure factor modulations, assuming that double diffraction is negligible. The electron diffraction pattern of a spinodally decomposed copper-titanium alloy shown in Figure 2 (Datta and Soffa, 1976) reveals the dominant <100> concentration waves that develop during the early stages of phase separation. The extinctions of the satellites at certain reciprocal lattice nodes (where $\vec{g} \cdot \vec{R} = 0$) show that the satellites arise primarily from *longitudinal displacive* waves induced by the concentration waves.

If the strain energy term in the free energy expression is negligible (small misfit) or if the elastic modulus is isotropic, the resultant microstructure will be isotropic, similar to the morphologies evolving in phase-separated glasses (Cahn and Charles, 1965; Cahn, 1965). In Figure 3, an isotropic spinodal structure developed in a phase-separated iron-chromium-cobalt permanent magnet alloy is clearly revealed by transmission electron microscopy. The two-phase mixture is interconnected in three dimensions and exhibits little or no directionality. The microstructure is comparable to the computer simulation of an isotropically decomposed alloy shown in Figure 4. On the other hand, in the microstructure shown in Figure 5, the dominant composition waves have developed preferentially along the <100> matrix directions to produce an aligned modulated structure in a copper-nickel-chromium alloy (Chou *et al.*, 1978). Its electron diffraction pattern would be similar to that shown in Figure 2. Because the homogeneous phase separation process is relatively structure-insensitive, the spinodal product is generally uniform within the grains up to the grain boundaries, and independent of such defects as dislocations, stacking faults, twins, *etc.*

Finally we should consider decomposition in the region near the *mean field spinodal*. In this region, the classical models for understanding both nucleation and spinodal decomposition break down quantitatively. The classical nucleation theory rests on the major assumption that the *only* nuclei to form are those whose barriers to formation, ΔG^*, are minima. At

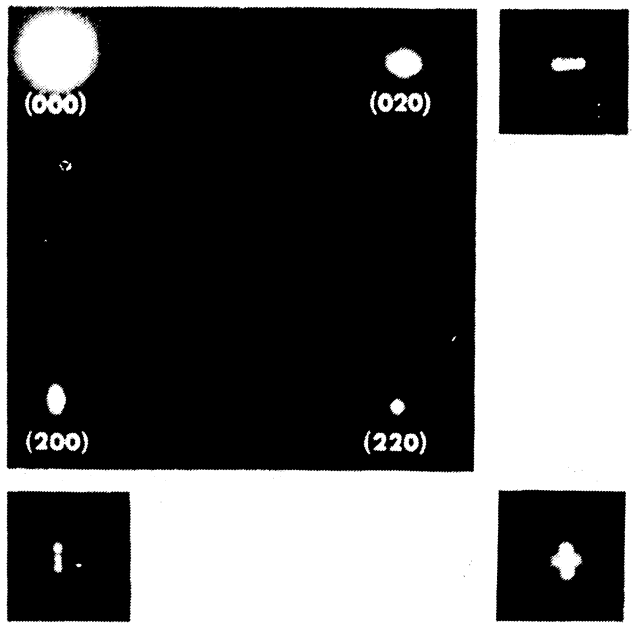

Figure 2. A [001] electron diffraction pattern taken from a Cu-4 wt/% Ti alloy aged 100 min at 400 C, showing <100> satellites flanking the fundamental reflections. Note the extinction of the [010] satellites at the (200) position and the [100] satellites at the (020) position, consistant with the presence of <100> longitudinal strain waves.

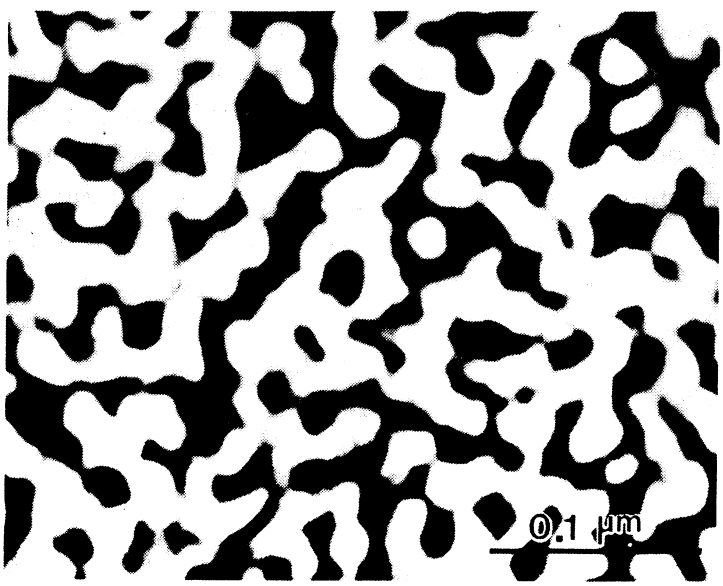

Figure 3. A transmission electron micrograph of Fe-28.5 wt/% Cr-10.6 wt/% Co alloy aged 4 hrs at 600 C. Note that the contrast appears to be isotropic and derives from structure factor variations.

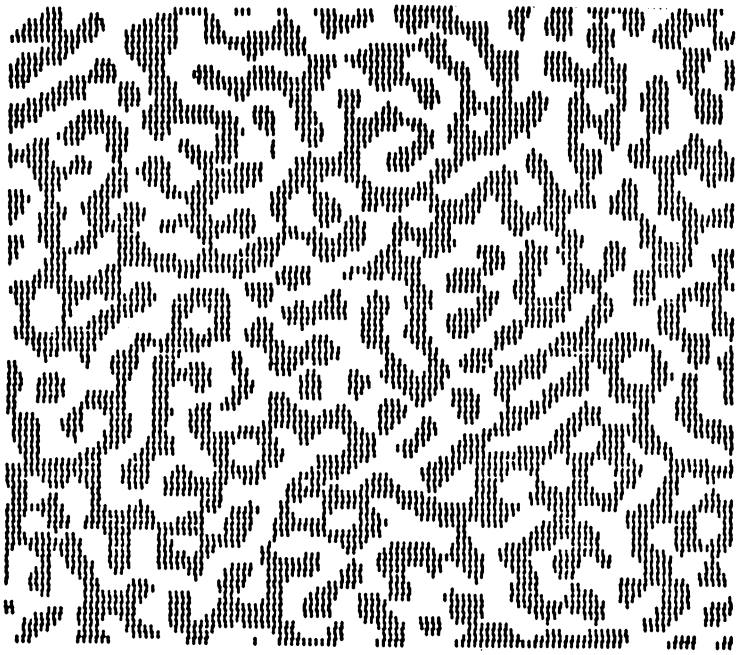

Figure 4. A computer simulation of an spinodally decomposed solution, exhibiting isotropic elasticity (after Cahn, 1965).

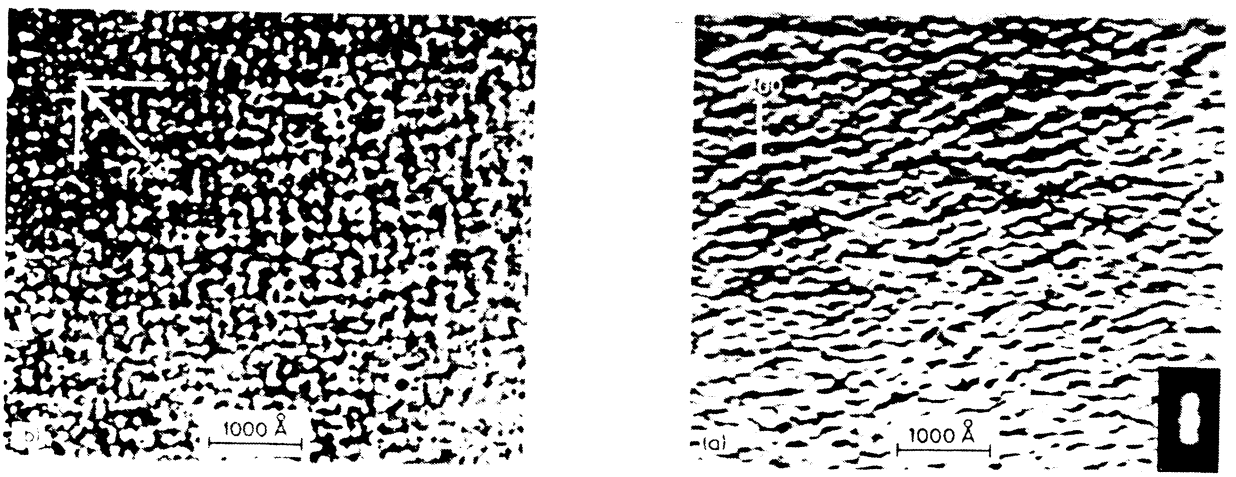

Figure 5. The microstucture of a Cu- 31.6 wt/% Ni-1.7 wt/% Cr alloy, aged at 650 C for 1 hr. The figure on the left is taken under diffraction conditions such that two sets of <100> modulations are visible. In the figure on the right, only one set of modulations is visible. This shows that the contrast derives from longitudinal displacive waves, induced by compositional modulations.

undercoolings near the mean field spinodal, such an assumption is unreasonable. Many decomposition paths exist with barriers of the order of 1-10 kT. These paths appear to be barrierless, because they can be readily surmounted by composition fluctuations induced by thermal agitation. Thus the decomposition process appears to be continuous in many aspects. However, this decomposition cannot be modeled quantitatively by classical spinodal theories, because the assumptions involved in these theories also break down as the spinodal is approached. Of course, the decomposition process occurs, whether we can model it or not! Recent advances in the theory of decomposition have been made along the lines of extending either the nucleation type approaches (cluster kinetics) to larger supersaturations or extending the spinodal decompositional approaches to smaller supersaturations. The common finding of all the theories is that there is not an abrupt transition between the two extremes in decomposition behavior as described above. Rather, the process changes progressively from nucleation-like behavior to spinodal like behavior through a region in which decomposition exhibits characteristics of both processes (Cahn and Hilliard, 1958; 1959; Binder *et al.*, 1978 and Aaronson and Russell, 1982).

3. ATOMIC ORDERING

3.1 Single Order Parameter

A simple phase diagram for atomic ordering of a bcc phase (A2) is shown in Figure 6. The high temperature disordered phase is stable at temperatures above the hatched line and *unstable* at temperatures below the line. In this case only first neighbor interactions have been taken into account. On cooling through the instability temperature, the disordered phase becomes unstable with respect to the formation of short wavelength composition waves, which are characteristic of the ordered structure. The ordering builds up throughout the entire system (homogeneous) and occurs without a thermodynamic barrier (continuous). The accompanying free energy *versus* composition curves at the temperature shown denotes that the disordered phase is unstable by inverted hatched lines. This instability is with respect to atomic ordering. The slopes of the curves are the same at the termination of lines of instability, since the transition is of *higher order*.

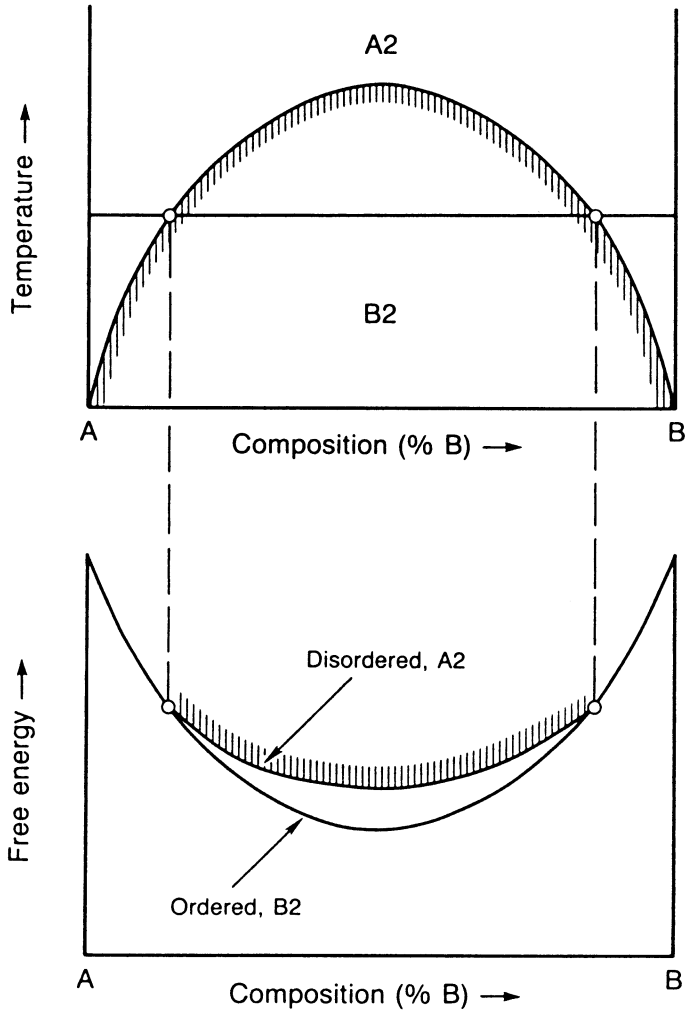

Figure 6. A schematic phase diagram and accompanying free energy *versus* composition diagram of a solution exhibiting a higher order atomic ordering reaction. The hatched lines denote where the solution is unstable with respect to (continuous) ordering.

3.2 Two Order Parameters

3.2.1 Higher Order Order/Disorder Transition

If second neighbor interactions are taken into account, the low temperature equilibrium state of off stoichiometric compositions must be two phase, since the ordered structure has opposite second neighbors (Ino, 1978; Kubo and Wayman, 1980). To minimize the energy in such cases, the solute atoms must segregate and then atomically order. The clustering of solute allows for the maximum number of similar *second* neighbors within the ordered phase. This shows that clustering and ordering are not opposite processes; in fact, they very often occur together in decomposition reactions (Soffa and Laughlin, 1982).

Figure 7 shows the phase diagram of the order/disorder system when the second neighbors interaction energies are taken into account. At low temperatures, the equilibrium state is two phase, one of which is the ordered B2 phase (CsCl, $Pm\bar{3}m$); the other is the disordered A2 phase (W,$Im\bar{3}m$). The line of higher order transitions intersects the miscibility gap at a *critical end point*. The free energy curves at temperatures T_3, T_2 and T_1 are shown in Figures 8, 9 and 10 respectively. At T_3 (Figure 8), the ordered phase breaks away at the composition denoted C_λ, the slopes of both free energy curves are identical at this point, while their curvatures are different. At the lower temperature T_2 (Figure 9), the ordered phase develops a miscibility gap. Spinodal decomposition of the ordered phase is now possible. At lower temperatures yet (T_1, Figure 10), the equilibrium consist of an ordered phase (B2) and a disordered phase, A2. Figure 10 can be used to delineate various decomposition paths. For solute compositions up to but less than C_λ, the disordered phase upon entering the two phase region is metastable with respect to the formation of the ordered phase; *viz.* the ordered phase must nucleate. For compositions between C_λ and C_s', the disordered phase first becomes unstable with respect to homogeneous ordering and then the ordered phase becomes metastable with respect to the formation of the equilibrium disordered phase. Finally, for compositions between C_s' and C_s'' the disordered phase at T_1 first becomes unstable with respect to the continuous formation of B2, which in turn is unstable with respect to phase separation into two ordered phases. Eventually one of the ordered phases disorders, as its composition becomes less than C_λ. The latter spinodal decomposition has been termed "conditional" by Allen and Cahn (1976), since it is contingent on the prior ordering of the disordered phase.

A limiting case of the *critical end point* diagram is shown in Figure 11. Here the critical *end point* has become a *tricritical* point, since the line of

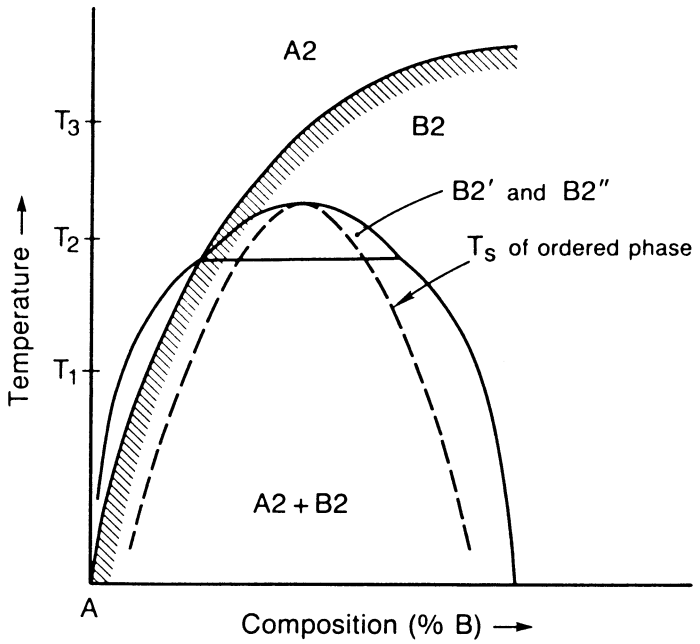

Figure 7. A schematic phase diagram of a solution exhibiting a *critical end point.* Within the two phase region, a quenched A2 solution could be either metastable or unstable with respect to phase separation. The spinodal region delineates instability with respect to phase separation contingent on prior atomic ordering, *i.e.* a conditional spinodal.

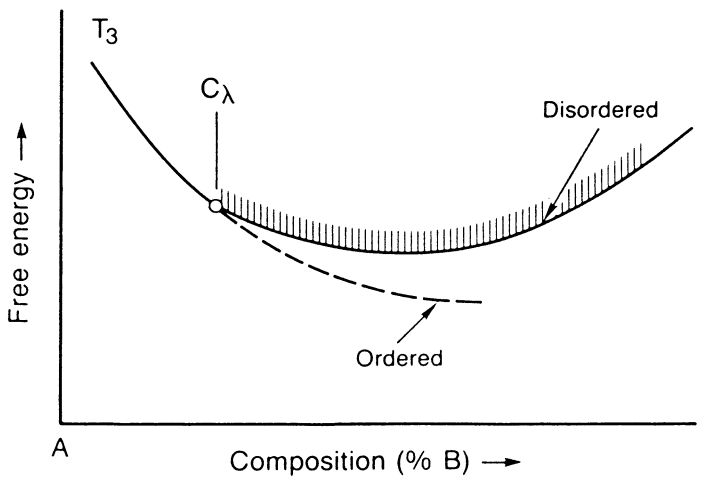

Figure 8. A schematic free energy *versus* composition diagram of the solution shown in Figure 7, at $T=T_3$. Note that the ordered solution is everywhere stable with respect to phase separation.

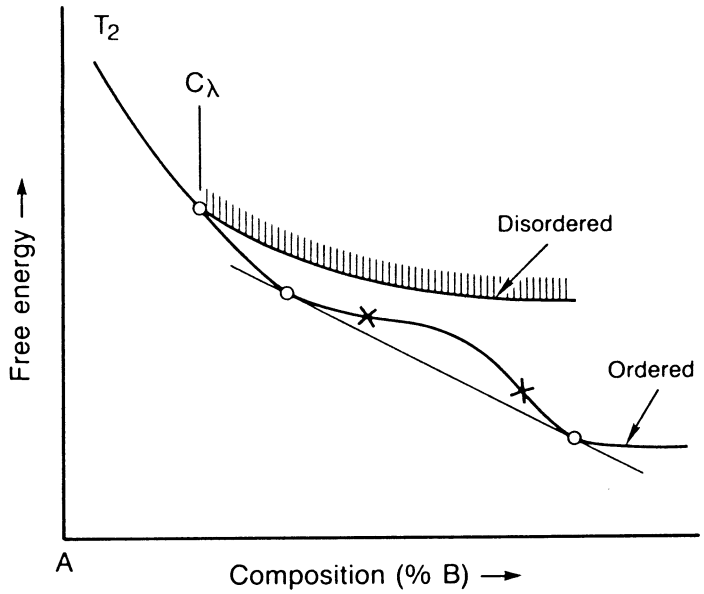

Figure 9. A schematic free energy *versus* composition diagram of the solution shown in Figure 7, at $T=T_2$. Note that the ordered solution exhibits an unstable region between the x's.

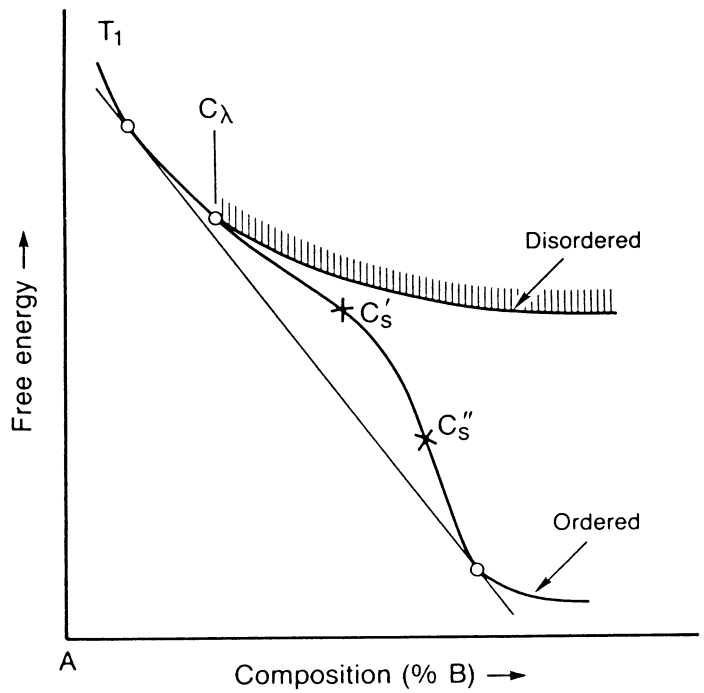

Figure 10. A schematic free energy *versus* composition diagram of the solution shown in Figure 7, at $T=T_1$. Note that the ordered solution exhibits an unstable region, and also that the equilibrium conjugate phases are ordered and disordered respectively.

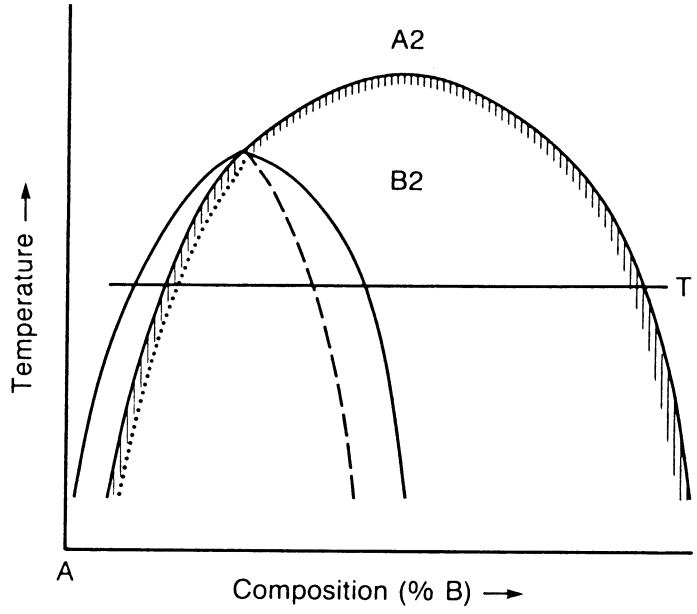

Figure 11. A schematic phase diagram of a binary system exhibiting a *tricritical point.* Here the line of higher order transitions terminates uniquely at the top of the two phase region. The dashed curve represents a spinodal line (G"=0) for the ordered phase, whereas the dotted line (coincident with the A2→B2 transition line) represents a limit of metastability (G" changes sign discontinuously from positive to negative).

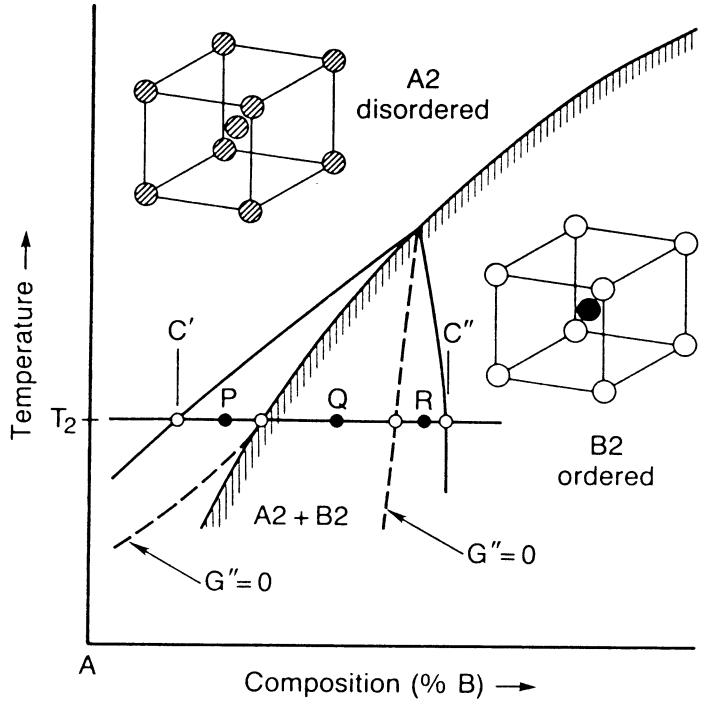

Figure 12. Region near the *tricritical point,* showing the emergence of a spinodal in the disordered solid solution at low temperature. Points P,Q and R represent initial states of a quenched solid solution, exhibiting different thermodynamic stabilities with respect to clustering and ordering.

higher order transitions is drawn so as to terminate uniquely at the critical point of the miscibility gap. As shown in the diagram, the instability of order now coincides with the instability for phase separation on the left hand side of the diagram. Importantly, the limit of metastability on the left represents a discontinuity of G", across which it changes sign abruptly, from positive to negative without going through zero.

We now look at the tricritical case in more detail. Figure 12 shows the region near the *tricritical point* and the free energy *versus* composition curve at T_2 is shown in Figure 13. T_2 is the temperature at which the spinodal of the disordered phase coincides with C_λ. As shown in Figure 12, below T_2 a region exists in which a quenched disordered phase is unstable with respect to phase separation into two disordered phases. This spinodal reaction will be followed by the continuous ordering of the solute-enriched phase.

Let us examine the decomposition paths of disordered solid solutions quenched to points P, Q and R, respectively. A disordered solution quenched to P is metastable with respect to the formation of the ordered B2 phase. A disordered alloy quenched to Q is unstable with respect to homogeneous, continuous ordering into a single order phase, Q'. This ordered phase is unstable with respect to spinodal decomposition into two ordered phases. Eventually, the composition of the solute depleted phase passes through the line of critical points, and it disorders. Finally, a disordered phase quenched to R is unstable with respect to homogeneous ordering to R'. The ordered phase is then metastable with respect to the formation of the disordered A2 phase. These three different decomposition paths all take the initially disordered phase into a state where disordered and ordered phases are in equilibrium.

3.2.2 First Order Order/Disorder Transformations

Spinodal processes occurring in solid solutions in conjunction with an apparent metastable or stable order/disorder transition thermodynamically of first order are not generally well understood. However, these continuous processes involving concomitant ordering and phase separation appear to be common in metallic and non-metallic systems. The following discussion is essentially after Kuikarni *et al.*, 1986 and Khachaturyan *et al.*, 1987.

Consider a metastable or stable phase diagram configuration in a binary system based on an fcc crystal structure as shown in Figure 14. The γ phase is an ordered phase which is a crystallographic derivative of the high temperature α solid solution; that is, the superstructure can be produced by a simple atomic rearrangement on the sites of the fcc lattice, thus reducing the

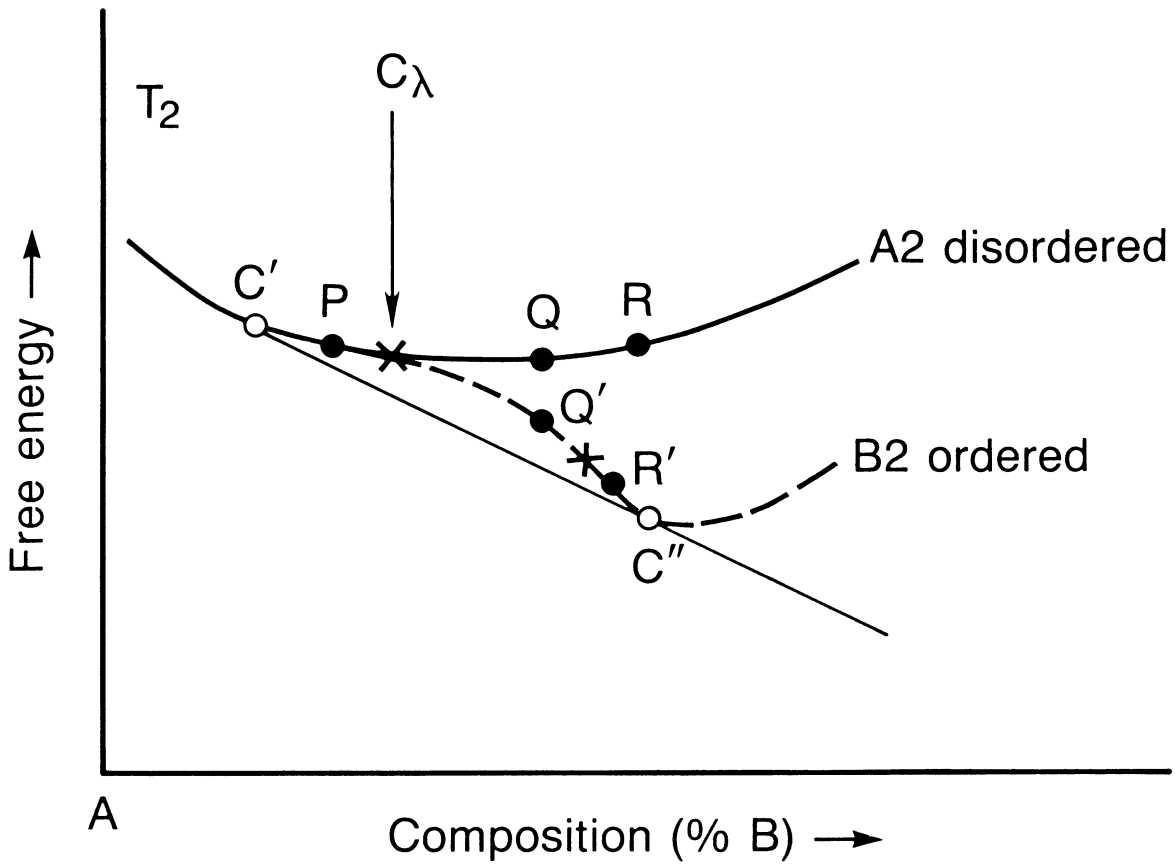

Figure 13. Free energy *versus* composition diagram at T_2, showing the disordered and ordered solutions corresponding to the states P, Q and R of Figure 12.

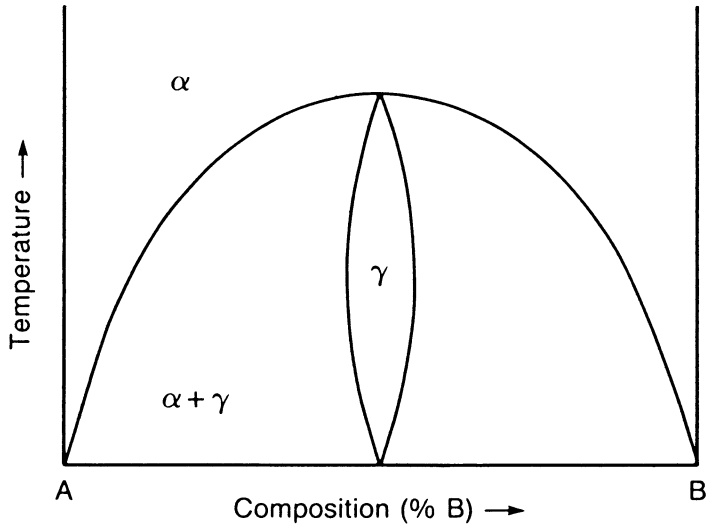

Figure 14. Binary system exhibiting a first order order/disorder reaction. Here, a stable two phase region exists at all temperatures below the critical temperature for the γ phase.

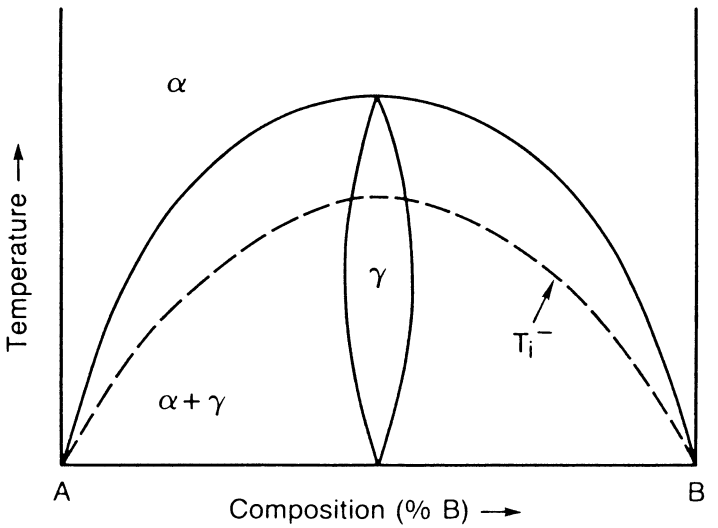

Figure 15. First order reaction showing the *locus* of ordering instability (T_i^-). Below T_i^- a quenched disordered phase will homogeneously or continuously order.

symmetry of the disordered phase. The ordered phase will have a stoichiometry A_xB_y, for example, A_3B or AB. It is well-known that at small departures from equilibrium the ordered phase can only emerge in an undercooled α phase phase by a heterogeneous reaction involving the nucleation and growth of small, highly ordered regions within a disordered matrix. This is termed "heterogeneous ordering". However, at large degrees of undercooling or large departures from equilibrium, the disordered phase can become thermodynamically unstable and continuously order by the progressive amplification of "ordering waves" uniformly throughout the system, *i.e.*, "homogeneous or continuous ordering". The homogeneous ordering reaction is the counterpart of spinodal decomposition in the scheme of reaction paths involving order/disorder processes. The continuous ordering process can occur for $T \leq T_i^{\cdot}$ where $T_i^{\cdot}$ is the "ordering instability temperature" on cooling. In this regime away from equilibrium, the phase transformation has many of the thermodynamic and kinetic properties of a second or higher order transition. See Figure 15.

The instability locus can be calculated thermodynamically in a straightforward manner using the method of concentration waves (Khachaturyan, 1978 and 1983) and is given by:

$$T_i^{\cdot} = \frac{-2V(\vec{k})c(1-c)}{k_B}$$

where $V(\vec{k})$ for the wave vector $\vec{k}$ is related to the Fourier transform of the pair interaction parameter

$$V_i = E^i_{AB} - \frac{1}{2}\left(E^i_{AA} + E^i_{BB}\right)$$

where E^i_{AB}, E^i_{AA} and E^i_{BB} are the AB, AA, and BB bond interaction energies in the i^{th} nearest-neighbor shell, respectively. Ordering instabilities are associated with "special points" in $\vec{k}$-space where the function $V(\vec{k})$ is an *extremum* (de Fontaine, 1975). Clustering instabilities are associated with the term V(0) in this formalism (Khachaturyan, 1978 and 1983).

Consider the free-energy *versus* composition schemes with decreasing temperature and associated phase diagram shown in Figures 16-19. The common tangent construction establishes the equilibrium compositions of the conjugate phases in the two-phase region in the usual manner. A solution of composition C_o rapidly quenched from T_o to T_1 would form the equilibrium $\alpha+\gamma$ two-phase mixture by nucleation and growth of the ordered γ phase within the supersaturated disordered phase (Figure 17). However, if an alloy of

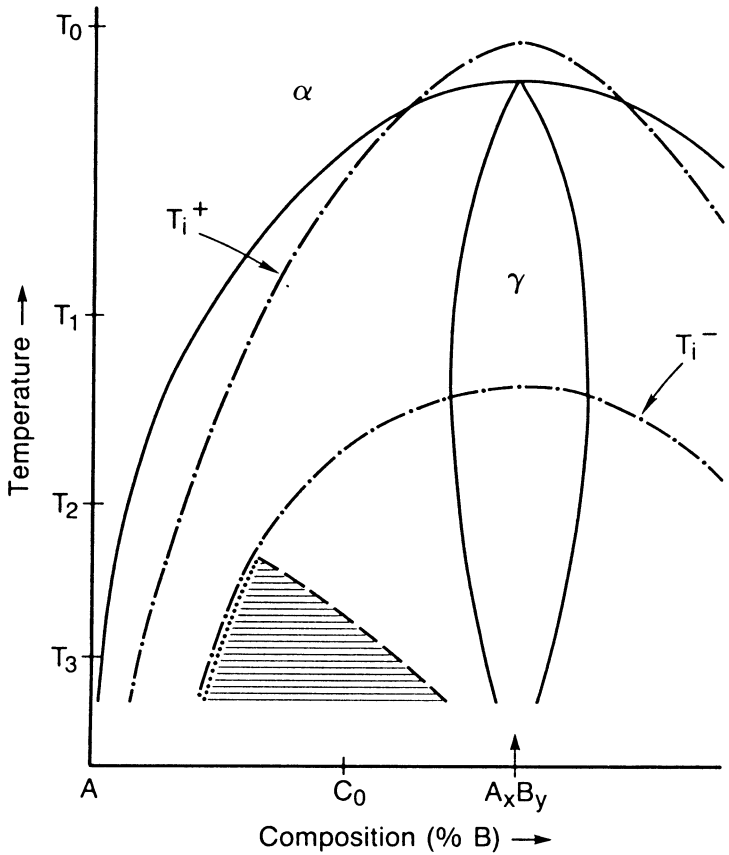

Figure 16. Schematic of a first order order/disorder phase diagram with various instability lines included. In the crosshatched region the homogeneously ordered phase is unstable with respect to phase separation. The *locus* T_i^+ is the instability line of the ordered phase with respect to disordering upon heating.

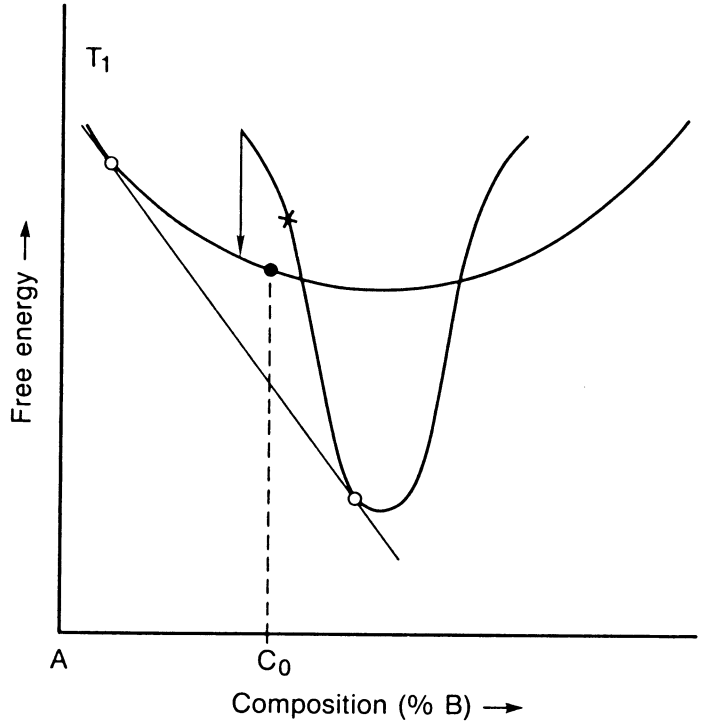

Figure 17. Schematic free energy *versus* composition diagram for the ordered and disordered phases at T_1. The arrow denotes the limit of stability of the ordered phase.

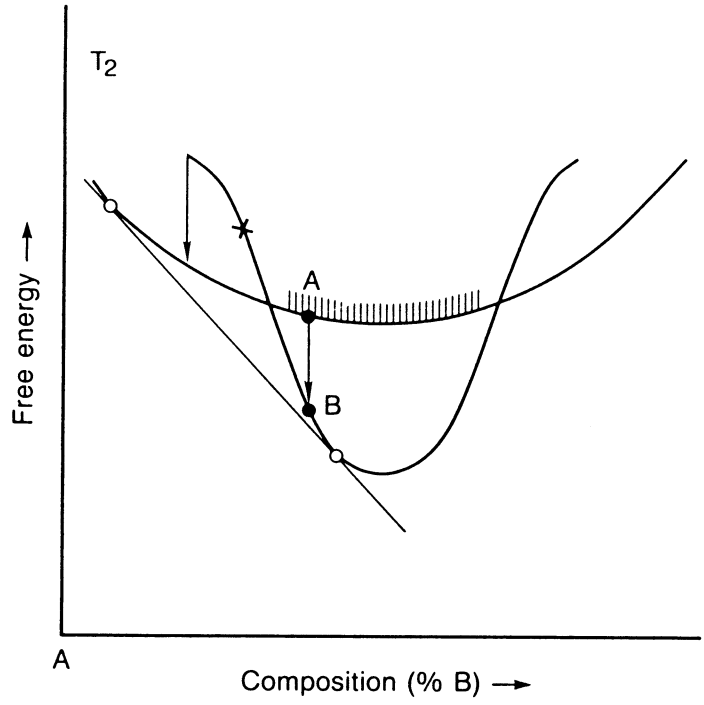

Figure 18. Schematic free energy *versus* composition diagram for the ordered and disordered phases at T_2. The hatched segment of the free energy curve for the disordered phase corresponds to solutions which are unstable with respect to continuous ordering.

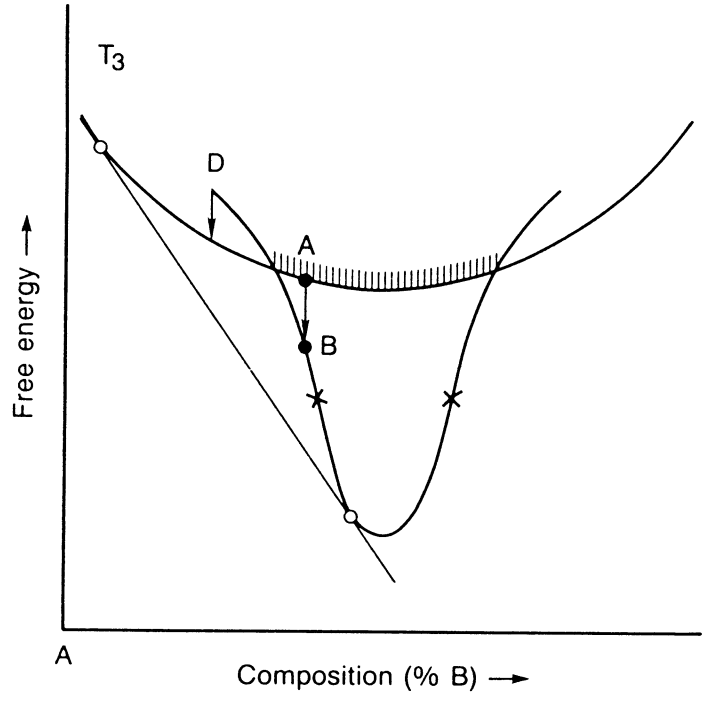

Figure 19. Schematic free energy *versus* composition diagram for the ordered and disordered phases at T_3. Note the appearance of a spinodal (G"=0) in the ordered phase and a region of thermodynamic instability with respect to phase separation contingent on prior atomic ordering.

composition C_o is quenched to the temperature T_2 from the single phase region, the free energy *versus* composition scheme shown in Figure 18 obtains. Here, another reaction path will occur. The hatched region of the α curve now delineates compositions which are unstable with respect to continuous ordering. The α phase will order homogeneously or continuously, bringing the free energy of the solution from point A to point B. The equilibrium two-phase mixture will now be produced by classical nucleation of disordered α within the ordered solution. See Figure 18.

Now consider the temperature T_3 and the free energy *versus* composition scheme shown in Figure 19. At T_3 the solution of composition Co is unstable with respect to ordering and the continuous ordering process will take the free energy from point A to point B. But the ordered state of the solution at B is unstable with respect to phase separation and will undergo spinodal decomposition or continuous phase separation. The compositions of the emerging phases move along the free energy curve for the ordered phase and at point D the solute depleted regions spontaneously disorder. This essentially defines a locus T_i^+ or an instability with respect to disordering on heating in the phase diagram (Khachaturyan *et al.*, 1987).

The different regimes of thermodynamic stability with respect to ordering, clustering and disordering can be summarized as follows: (See Figure 16) In the cross-hatched region a conditional spinodal reaction can occur in the ordered phase contingent on the prior ordering of the solution. The supersaturated states in the cross-hatched regions are actually thermodynamically unstable with respect to ordering and then clustering.

Interesting variations in conjunction with two fundamentally first order transformations are shown in Figures 20a and 20b. All supersaturated or non-equilibrium undercooled states which fall in the cross-hatched region in Figure 20a are unstable with respect to continuous ordering and phase separation within the ordered phase. The monotectoid configuration derives from a miscibility gap in the ordered phase. At $T=T_1$ the free energy *versus* composition diagram of the ordered phase exhibits two regimes of negative curvature as shown in Figure 21. At lower temperatures the regimes converge and the free energy *versus* composition diagram at T_2 is as shown in Figure 22. A metastable miscibility gap can also occur in the ordered phase, and produce the metastable diagram shown in Figure 20b.

It is also possible that the disordered phase could be unstable with respect to phase separation at higher temperatures, with ordering occurring at low temperatures as shown in Figure 23a. This produces a syntectoid isotherm

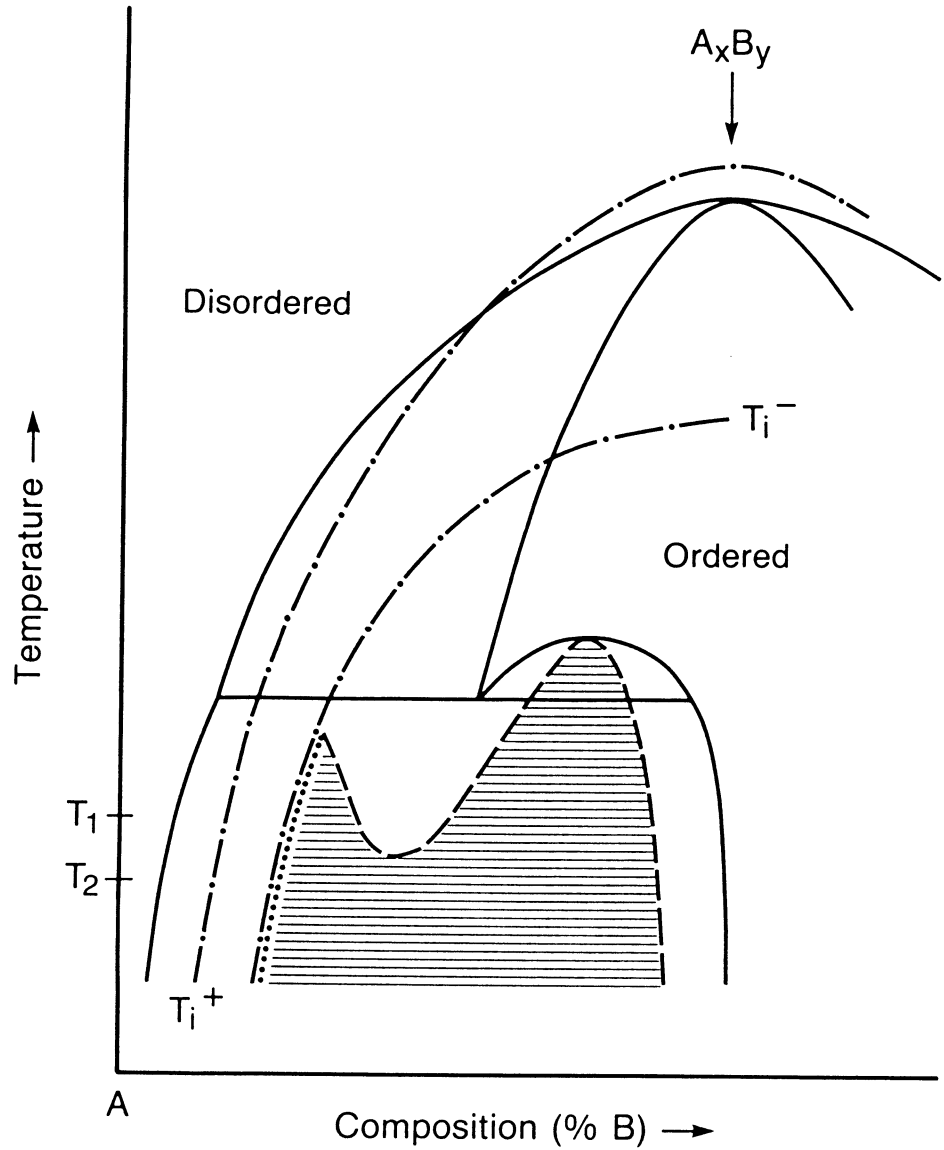

Figure 20a. Phase diagram configuration showing a monotectoid reaction involving the ordered and disordered phases. The crosshatched region denotes the region of thermodynamic instability with respect to phase separation.

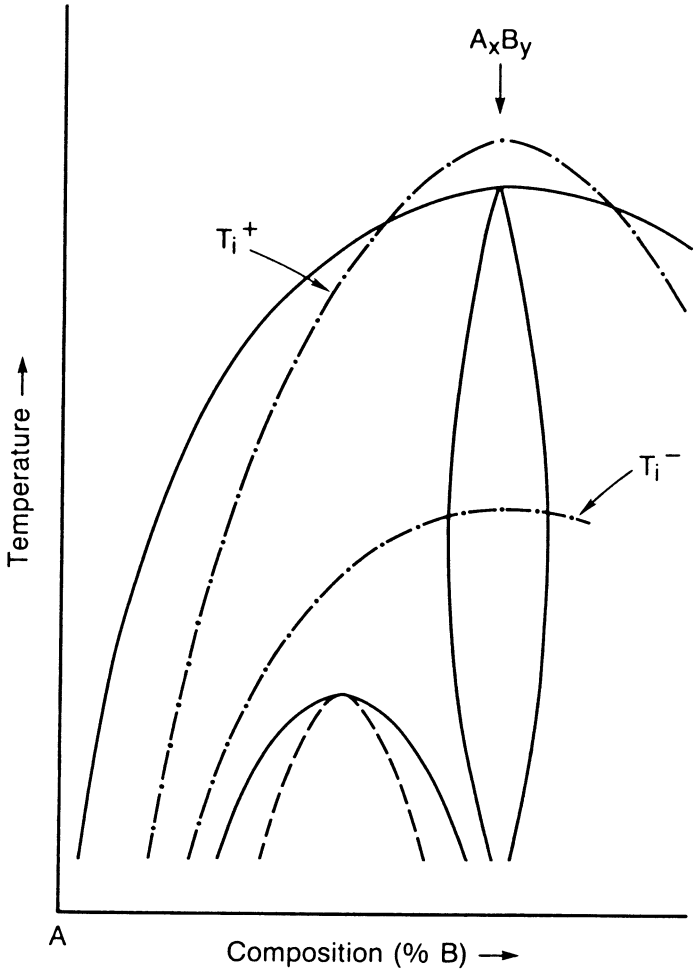

Figure 20b. A phase diagram for a first order order/disorder reaction showing a metastable miscibility gap in the homogeneously ordered phase.

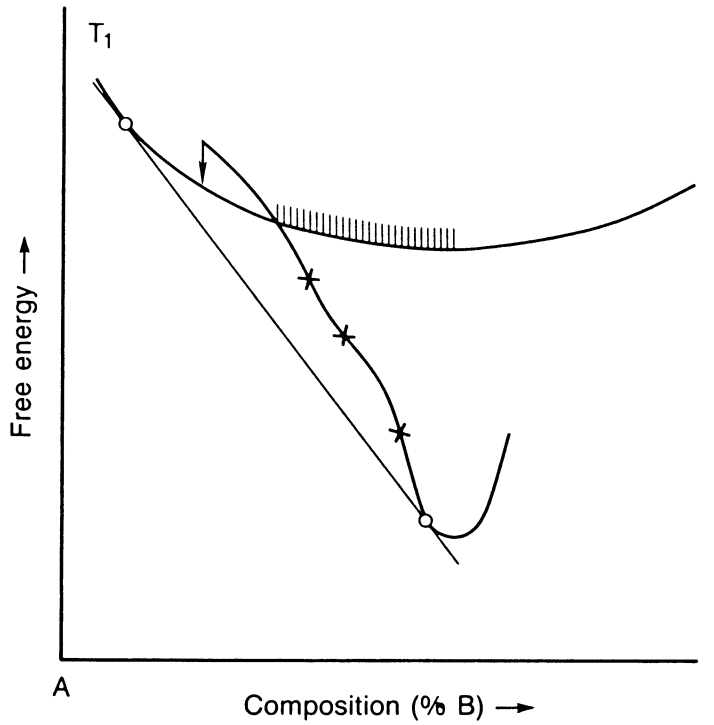

Figure 21. Free energy *versus* composition diagram at T_1 for the phase diagram shown in Figure 20a. Note the two regions of negative curvature appearing in the free energy curve of the ordered phase.

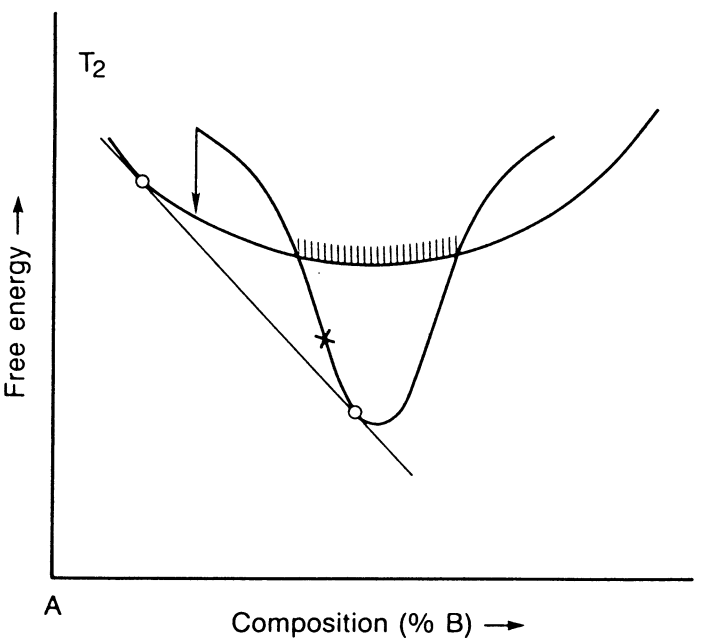

Figure 22. Free energy *versus* composition diagram at T_2 for the phase diagram shown in Figure 20a. Note that the two spinodal regions have merged.

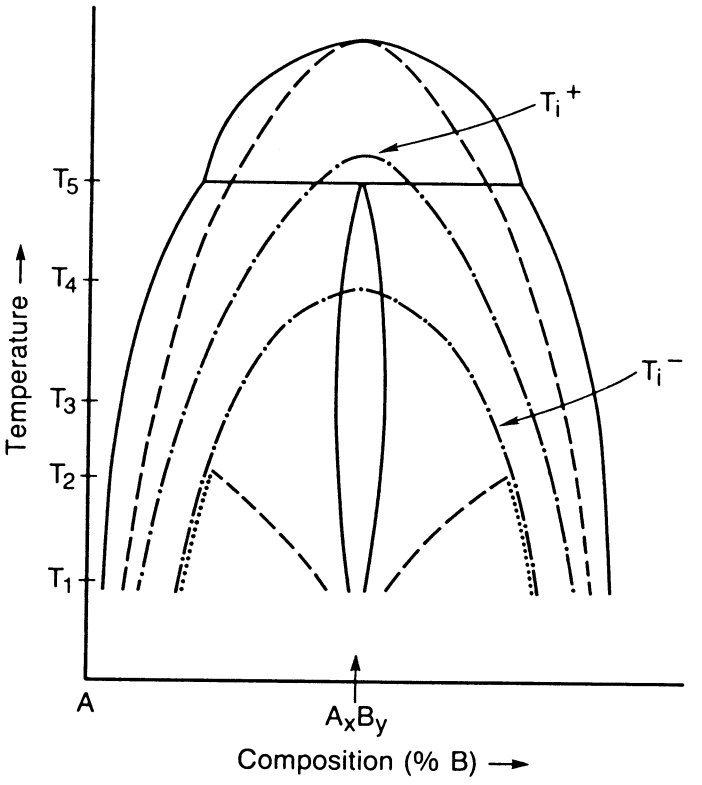

Figure 23a. Schematic phase diagram showing a miscibility gap in the disordered phase at higher temperatures and a first order order/disorder reaction at lower temperatures, combining to produce a *syntectoid* reaction isotherm. The various clustering and ordering instabilities have been included.

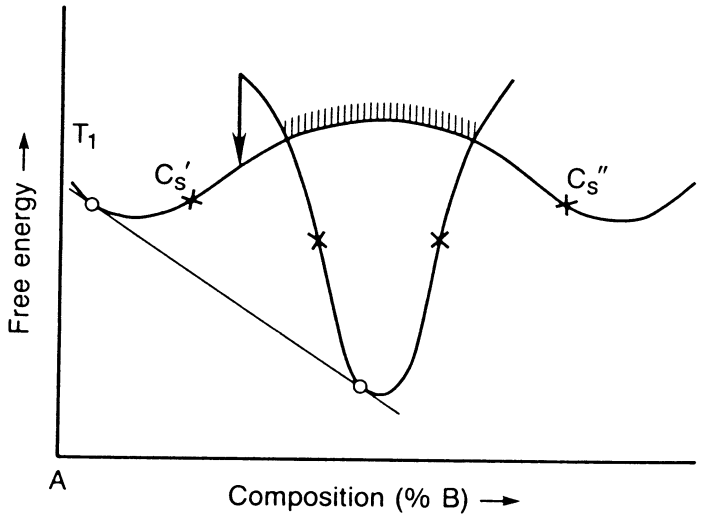

Figure 23b. Free energy *versus* composition diagram at T_1 for the phase diagram shown in Figure 23a. This free energy scheme allows for various reaction paths involving clustering and ordering.

at T_5. The free energy *versus* composition diagram at temperature $T=T_1$ is shown schematically in Figure 23b. Various reaction paths involving clustering and ordering can occur. If the high temperature, disordered phase α of composition just to the right of C_s' is quenched from the single phase region to produce a supersaturated state, it is unstable with respect to phase separation into two disordered phases. The solute-enriched regions will continuously order to γ beyond the point where the cross-hatching begins, and a two-phase mixture consisting of a disordered α phase and an ordered phase A_xB_y will obtain at equilibrium. The supersaturated state inside the hatched region, on the other hand, is unstable with respect to continuous ordering and phase separation; however, short-range atomic exchange will rapidly bring the solution to the ordered state. The ordered solution will spinodally decompose into two ordered phases if it is within the range of negative curvature with the solute-depleted regions spontaneously disordering at the composition where the arrow points downward. Again a two-phase mixture consisting of a disordered and an ordered phase is established at equilibrium. If the ordered phase is outside of the range of negative curvature it is metastable with respect to formation of a second phase and the disordered phase will nucleate within the supersaturated ordered phase.

In Figures 23c and 23d the free energy *versus* composition curves are displayed for the higher temperatures T_2 and T_3. At temperatures below the special temperature T_2, the ordered phase exhibits a region of instability with respect to phase separation. It is interesting to note that at the higher temperature T_3, solutions with compositions on the free energy curve for the disordered phase which are initially thermodynamically unstable with respect to both clustering and ordering can become metastable with respect to clustering *after* undergoing continuous ordering. The continuous ordering reaction will occur faster because of the shorter diffusional distances involved in the process. Thus, a supersaturated solid solution can initially be unstable with respect to both ordering and phase separation, but be rendered metastable with respect to phase separation by a prior ordering process. The metastable ordered state will precipitate a disordered phase by a classical nucleation process.

In Figure 20, the ordered phase was shown to exhibit a miscibility gap which produced a monotectoid configuration. A different monotectoid configuration can arise if the disordered phase exhibits a miscibility gap, as shown in Figure 24. It has been suggested that this configuration occurs in the commercially important Al-Li alloy (Gayle and Vander Sande, 1984).

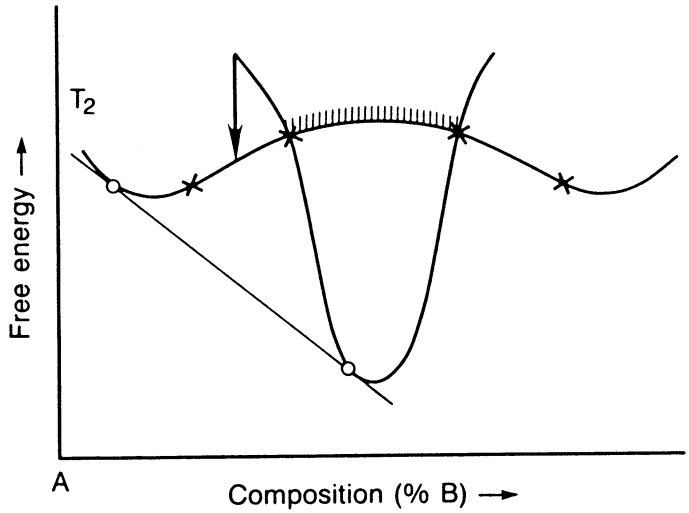

Figure 23c. Free energy *versus* composition diagram at T_2 for the phase diagram shown in Figure 23a. At this special temperature a region of instability with respect to phase separation begins to appear.

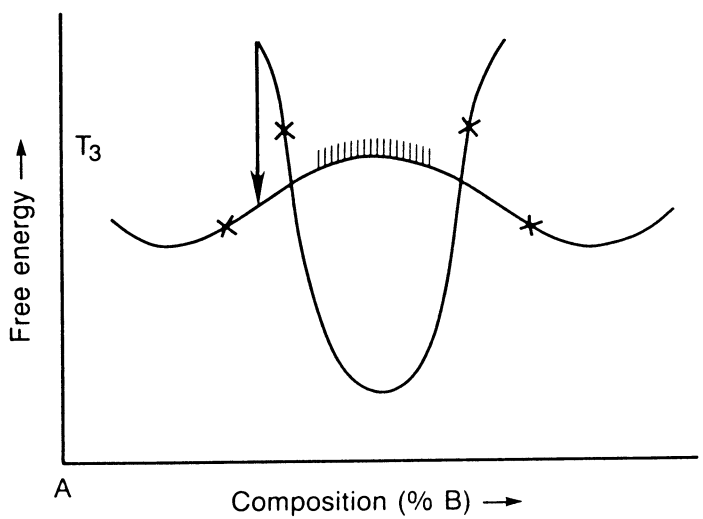

Figure 23d. Free energy *versus* composition diagram at T_3 for the phase diagram shown in Figure 23a. Note the limited range of compositions on the free energy curve of the disordered phase which exhibit ordering instabilities.

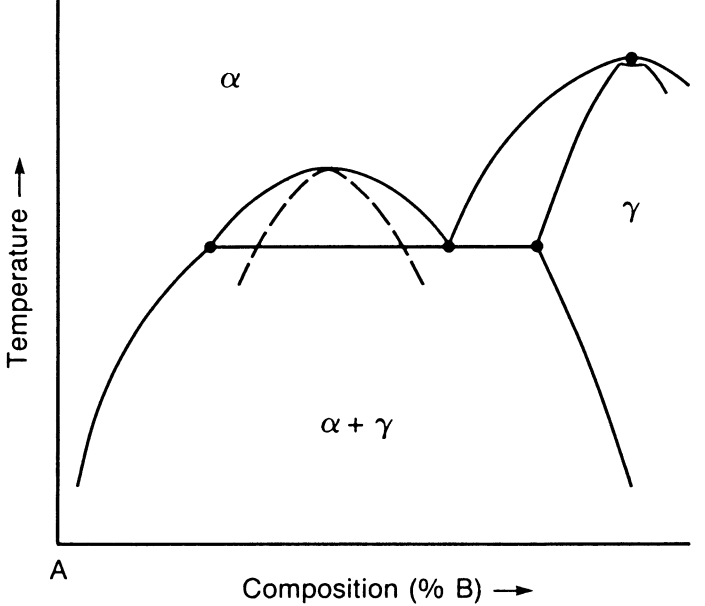

Figure 24. Monotectoid configuration associated with the ordered phase and a miscibility gap in the disordered phase.

4. MAGNETIC ORDERING

4.1 Introduction

The interaction of lines of higher order transformations associated with magnetic and/or atomic ordering with the usual first order boundaries in phase diagrams can produce unusual configurations of heterogeneous equilibria (Meijering, 1963, Miodownik, 1982 and Inden, 1982). Also, these effects can exert a significant influence on the variation of the free energy curve of a given phase with composition and temperature and thus markedly affect the thermodynamic stability of single phase states and the reaction paths leading to multi-phase states accessible to the system (Nishizawa *et al.*, 1979; Lin and Chang, 1987). The magnetic transitions (e.g. ferromagnetic, antiferromagnetic) involving ordering of elementary moments/spins require no mass transport and cannot be suppressed by rapid quenching. Also, magnetic contributions to the free energy can be quite large and thus these higher order transitions are expected to have an unavoidable primary influence on the phase diagram configurations and transformation mechanisms. Higher order/continuous atomic ordering processes which in principle, of course, can produce similar thermodynamic changes (see above) in the phase equilibria require at least short range atomic exchanges and thus can be suppressed by rapid cooling producing unstable or metastable disordered states. Many interesting effects are expected resulting from the simultaneous and synergistic effect of magnetic and atomic order. An important result of the interplay of these various influences on free energies of different phases is the appearance of multi-critical points and unusual critical point and miscibility gap configurations (Allen and Cahn, 1982).

4.2. Miscibility Gaps in Ferromagnetic Binary Systems

A simple but instructive example to use to begin our discussion is the *magnetically induced miscibility gap and tricritical point* appearing in a binary system as a result of the magnetic contributions to the free energy of the solid solution. Consider a binary fcc system which essentially forms an ideal solution with respect to atomic or chemical interactions, but one of the components, A, is ferromagnetic and exhibits a variation of the Curie temperature with concentration of the non-ferromagnetic component as shown in Figure 25. In the absence of magnetic contributions to the binary solution the face-centered cubic components form a complete series of solid solutions over the temperature range of interest and the free energy *versus* composition curve at a given temperature is everywhere concave upward as shown in Figure 26. However, if the influence of the magnetic transition on the solution thermodynamics is included, the free energy curves will show a markedly different behavior with decreasing temperature illustrated schematically in

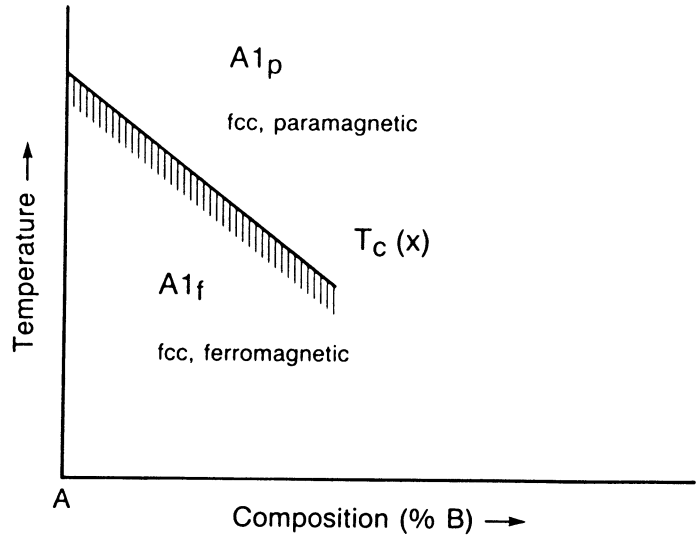

Figure 25. Schematic diagram showing the variation of the Curie temperature with composition in a binary system.

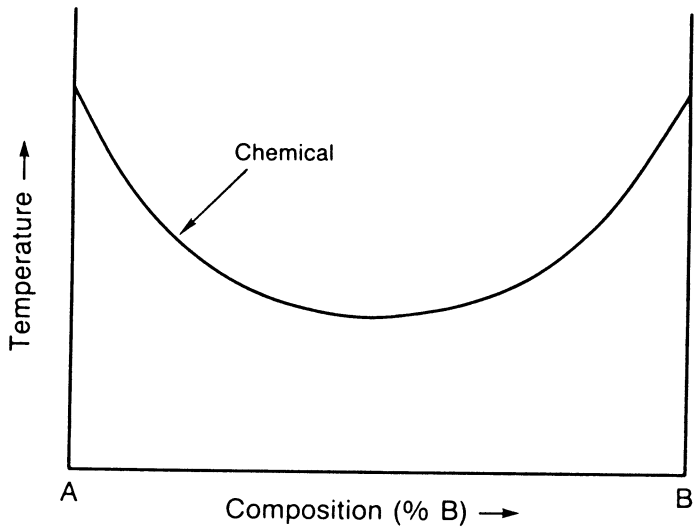

Figure 26. Free energy *versus* composition curve for a binary solution for which the chemical free energy exhibits nearly ideal behavior.

Figure 27. This variation of the free energy of the solutions rich in the ferromagnetic species results in a two-phase region at some critical temperature as shown in Figures 27b and 28. The Curie line ends at a sharp critical point T_c', a so-called *tricritical point.* Below the tricritical point a two phase region appears in which the conjugate phases are a ferromagnetic phase $A1_f$ enriched in the ferromagnetic component and a paramagnetic phase $A1_p$, enriched in the non-magnetic component. It should also be noted that the magnetically induced miscibility gap gives rise to a *spinodal curve* (G"=0) and a limit of metastability separating metastable and unstable single phase states. The extension of the Curie line produces a locus along which the second derivative of the free energy with respect to composition changes sign abruptly from negative to positive with increasing concentration of B - a limit of metastability. However at lower temperatures, a spinodal curve (G"=0) for the paramagnetic/disordered phase appears associated with the free energy *versus* composition scheme shown in Figure 29. (Compare with Figure 12.)

Above the "break away" temperature where the spinodal appears in the disordered phase only magnetically long range ordered single phase states (*ferromagnetic*) can be unstable with respect to phase separation and exhibit spinodal decomposition. However, below the "break away" temperature, single phase short range order paramagnetic states above the Curie temperature, $T_c(x)$, can spinodally decompose.

Figure 30 shows several alloys, and two aging temperatures within the two phase region. Note that if one were monitoring the decomposition behavior of solutions over a composition range within the two phase region of the phase diagram, using a technique which is sensitive to compositional changes as well as magnetic ordering (e.g. Mössbauer spectroscopy, neutron diffraction, *etc.*) the following reaction paths must be recognized and distinguished.

1. A solution of composition X_1 when quenched rapidly to temperature T_A results in the production of a single phase state at point Q (see Figure 30). This phase is magnetic, $A1_f$, and is unstable with respect to the formation of the paramagnetic phase $A1_p$ *via* continuous phase separation; *i.e.*, spinodal decomposition into two *ferromagnetic* phases occurs, the one which is enriched in the non-magnetic component eventually becoming *paramagnetic.*

2. A solution of composition X_2, on the other hand, when quenched to T_A - (i.e. point R) is *metastable* with respect to the formation of the *paramagnetic* phase; the paramagnetic phase will form by a nucleation and growth process, either homogeneously or heterogeneously, depending on the specific energy considerations.

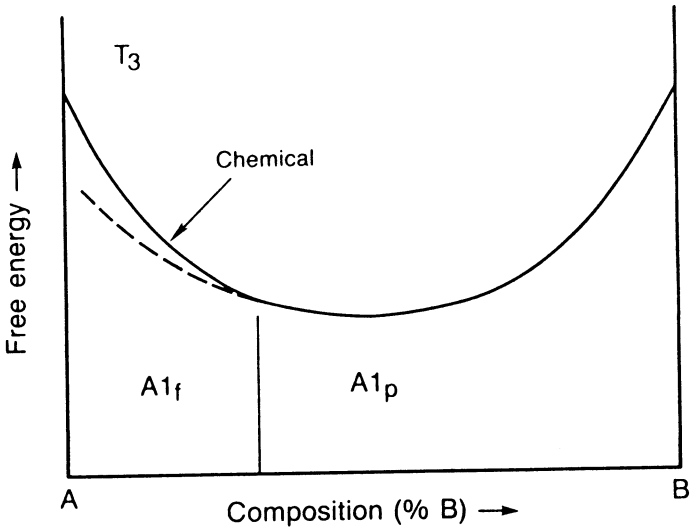

Figure 27a. Free energy *versus* composition curve for a binary solution showing the lowering of the free energy of the ferromagnetic phase over a range of compositions.

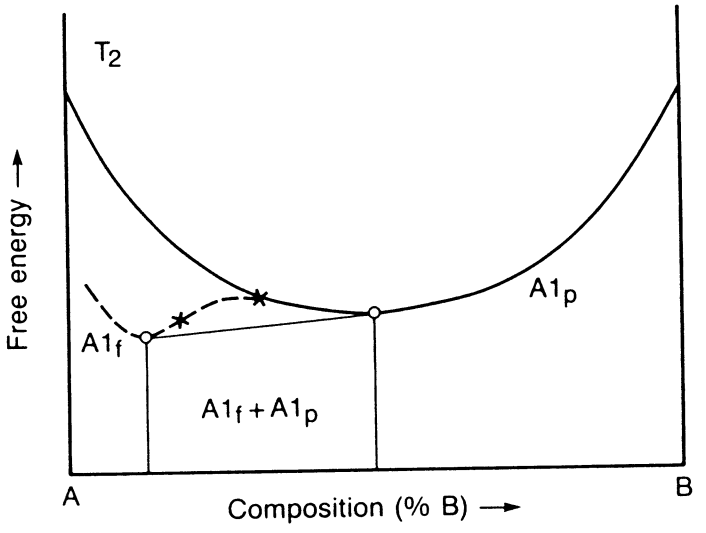

Figure 27b. Free energy *versus* composition curve for a binary solution showing the formation of a two phase region resulting from the magnetic contributions to the solution thermodynamics.

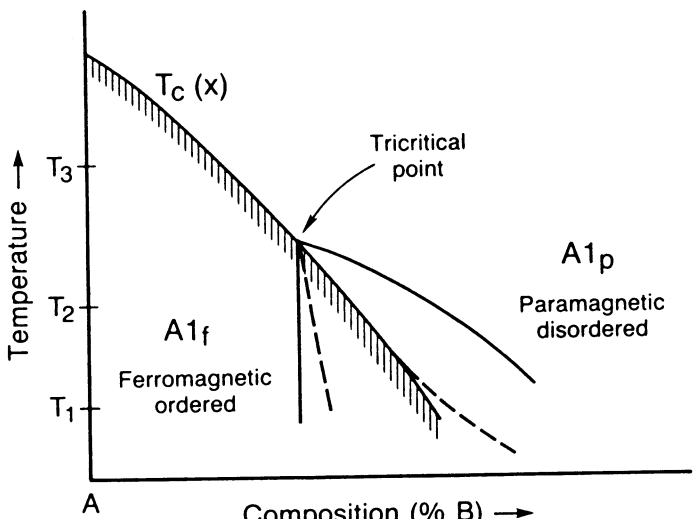

Figure 28. Magnetically induced two phase region and a *tricritical* point. Free energy *versus* composition curves at the temperatures T_2 and T_3 are shown in Figures 27a and 27b.

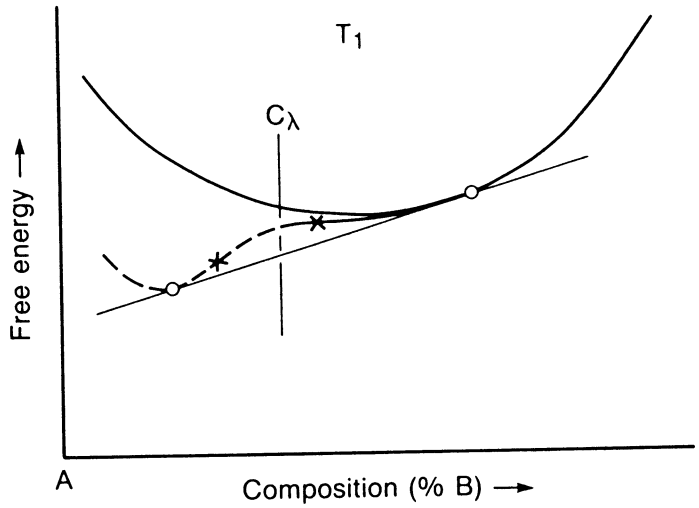

Figure 29. Free energy *versus* composition curve for the phase diagram shown in Figure 28 showing the emergence of a spinodal in the paramagnetic phase.

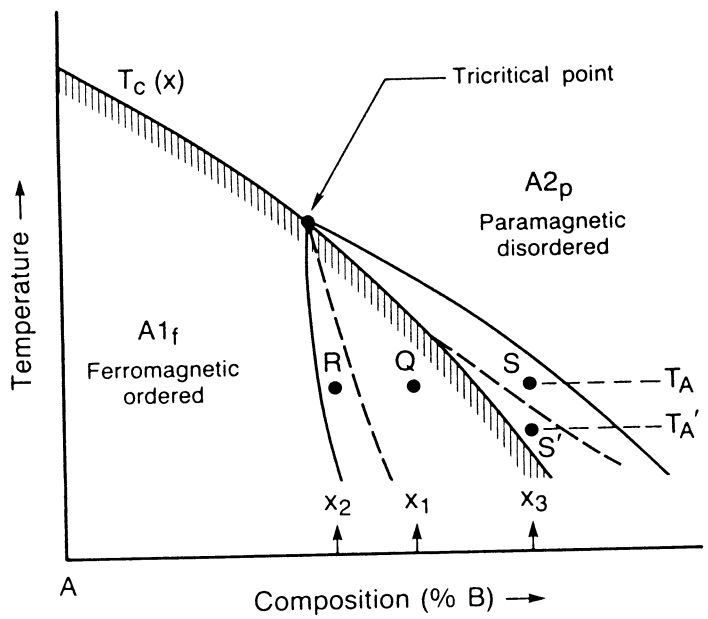

Figure 30. A phase diagram exhibiting a *tricritical* configuration and points Q, R and S representing different initial non-equilibrium states.

It should be noted that in both of these cases, the initial single phase state is *ferromagnetic*, because the spin ordering occurs immediately as the temperature falls below the Curie line ($T_c(x)$).

3. A solution of composition X_3, when quenched to T_A (point S) initially remains paramagnetic, being metastable with respect to the formation of the *ferromagnetic* phase, $A1_f$. At this temperature, the *ferromagnetic* phase can form only by means of nucleation and growth. If, however, the temperature is lowered to T_A' (S'), the single phase $A1_p$ is unstable with respect to continuous phase separation, *viz*, spinodal decomposition. Two *paramagnetic* phases initially form; one is enriched in the nonmagnetic component, B, and the other is enriched in the magnetic component, A. The regions that are enriched with the magnetic component become *ferromagnetic* as their composition crosses the Curie line.

It should be noted that the final state of each of the alloys discussed above is the same: namely a two phase mixture of *paramagnetic* and *ferromagnetic* phases. Only the paths to the equilibrium state varied. Of course, such differences would give rise to different microstructures, and possibly to different physical and mechanical properties of the transformed alloy.

4.3 Further Examples Including Magnetic Transitions

An example of a eutectoid*** diagram exhibiting a *tricritical* point is shown in Figure 31. This configuration seems to be particularly important in the Fe-Ni system and plays a central role in the behavior of the so called INVAR alloys as well as in the microstructural development in meteorites (Lin and Chang, 1987, Reuter, 1987).

Two further examples of the intersection of magnetic transitions with first order phase boundaries are shown in Figures 32 and 33. In Figure 32, the interaction of the magnetic transition with a chemical gap produces a *critical end point* and only a slight distortion of the phase boundary. The metastable extension of the Curie line is shown to produce a *metastable tricritical point* and a significant convolution of the spinodal curve. In Figure 33, the magnetic contribution to the free energy produces a *stable tricritical* point and attendant magnetically induced two-phase region which terminates on a monotectoid reaction isotherm. Again we see that the magnetic transition pulls the chemical spinodal upward producing the contorted regions of instability.

*** This diagram would be denoted as a monotectoid if the lowering of the symmetry of the γ_1 phase on magnetic ordering were ignored.

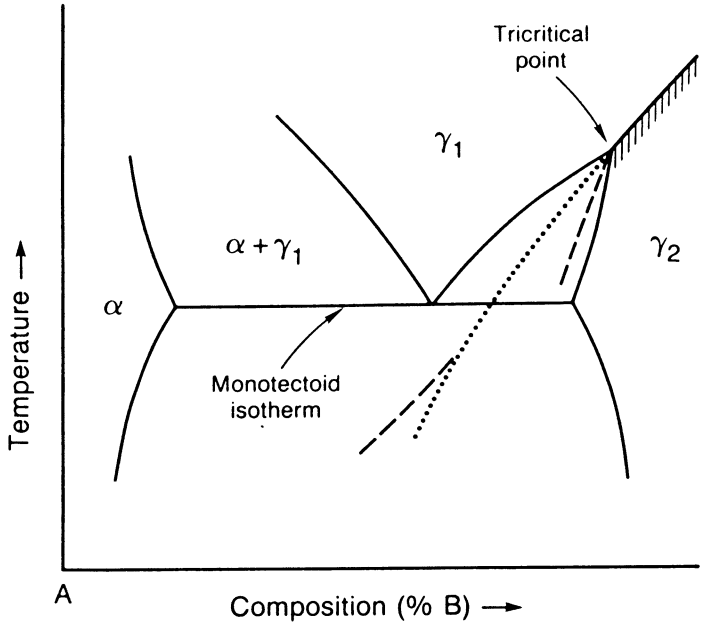

Figure 31. Eutectoid configuration associated with a *tricritical* point in a binary system.

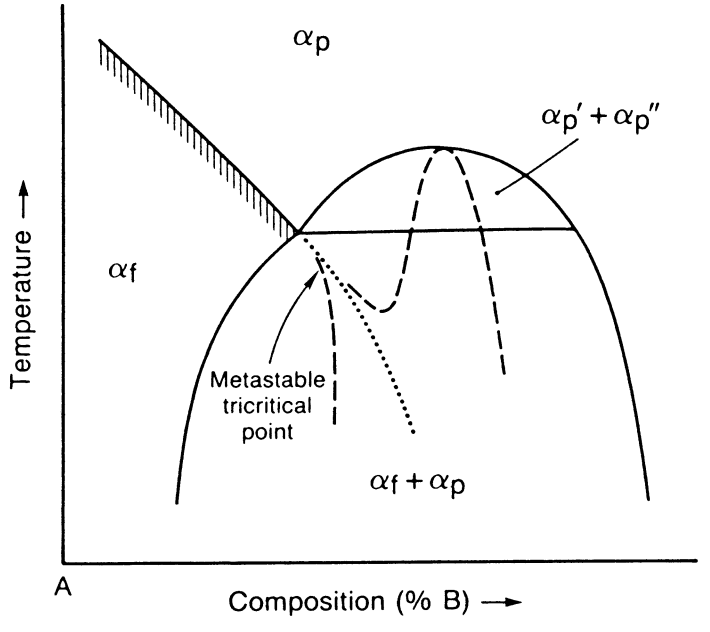

Figure 32. Interaction of a magnetic transition with a chemical miscibility gap producing a critical end point and a metastable *tricritical* point.

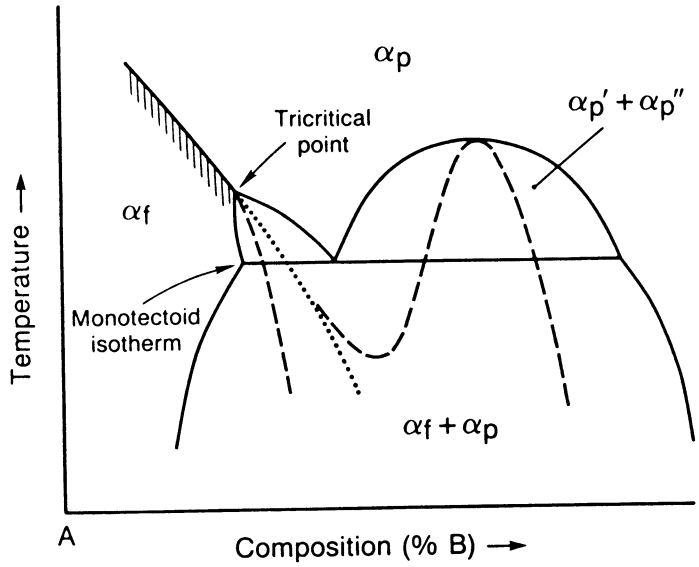

Figure 33. Interaction of a magnetic transition with a chemical miscibility gap producing a stable *tricritical* point and associated monotectoid isotherm.

5. BICRITICAL AND TETRACRITICAL POINTS

5.1 Introduction

The importance of multicritical phenomena in understanding phase equilibria and the transformation behavior of real systems with various ordering tendencies has been recognized over the past decade. (Griffiths, 1970; 1974; Allen and Cahn, 1982; de Fontaine, 1979). Allen and Cahn (1982) have discussed multicritical points in alloys based on a simple Landau-type free energy expansion and have characterized the essential features of bicritical, tricritical, and tetracritical points.

5.2 Bicritical Points

If we consider systems in which both magnetic ordering and atomic ordering ("higher order") can occur, the intersection of the two lines of criticality in a temperature *versus* composition diagram gives rise to a special multicritical point. If the phase which is produced by the combination of *both* ordering processes is *not* stable at low temperatures, the point of intersection is denoted a *bicritical* point. Such a diagram is shown in Figure 34. Here the *bicritical* point can be seen to exist at the top of the two phase region consisting of the different ordered phases. In this example, the paramagnetic bcc phase ($A2_p$) can order magnetically to the ferromagnetic phase $A2_f$ or atomically to the paramagnetic phase $B2_p$. These two phases form the two phase region below the *bicritical* point. The extensions of the ordering instability lines are also denoted in the diagram. A free energy *versus* composition curve which obtains for temperatures below the bicritical point is shown in Figure 35. Here it can be seen that the doubly ordered phase (ferromagnetic $B2_f$) is always unstable with respect to phase separation into two "singly" ordered phases ($A2_f$ and $B2_p$).

An interesting variant of a phase diagram containing a *bicritical* point along with the corresponding free energy *versus* composition curve is shown in Figure 36. Here, the doubly ordered phase becomes stable at low temperatures and a two-phase region between $B2_p$ and $B2_f$ is formed. The extension of the atomic ordering instability emerges from the two phase region producing the isotherm separating the $A2_f$ + $B2_f$ regions. Also, it should be noted that above this isotherm the doubly ordered phase is metastable over a limited temperature or composition range and a spinodal line appears.

An important metallurgical system which apparently exhibits a *bicritical*

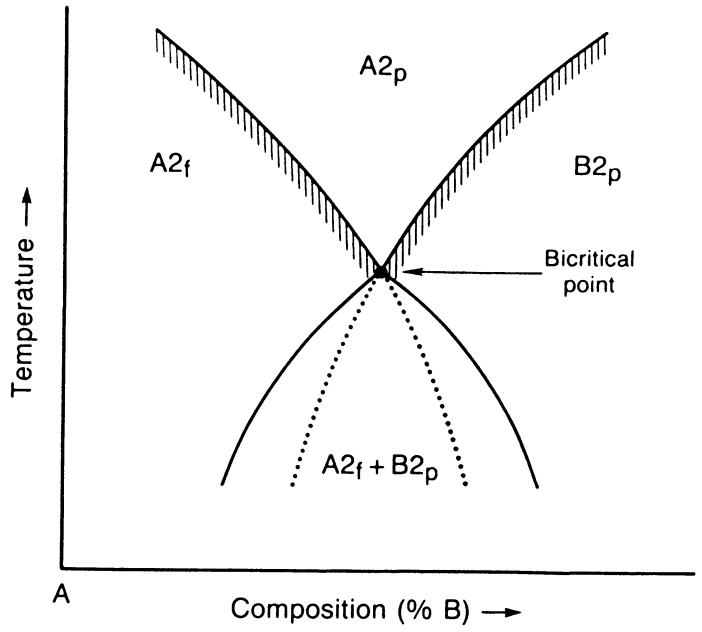

Figure 34. Bicritical point in a binary phase diagram deriving from two ordering tendencies, namely magnetic ordering and atomic ordering. Note that the extensions of the higher order transition lines project into the two phase region.

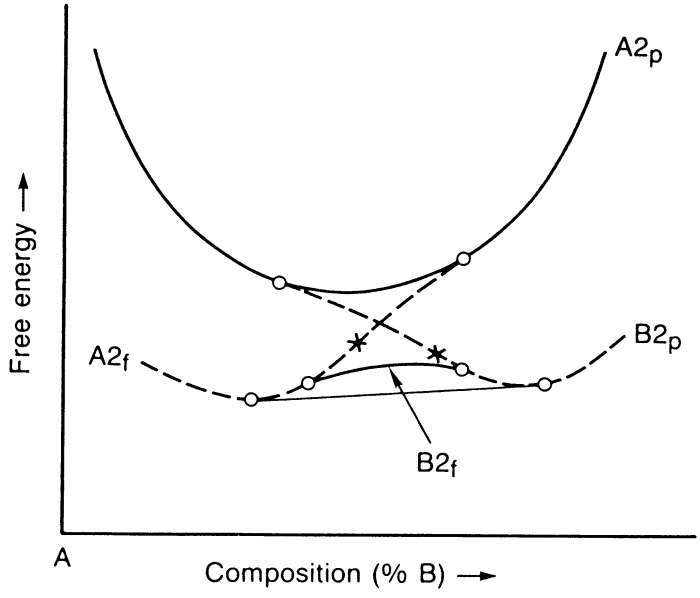

Figure 35. Free energy *versus* composition diagram for a temperature below the *bicritical* point. The common tangent denotes the equilibrium between conjugate phases $A2_f$ and $B2_p$. Note that the doubly ordered phase, $B2_f$, is thermodynamically unstable with respect to phase separation.

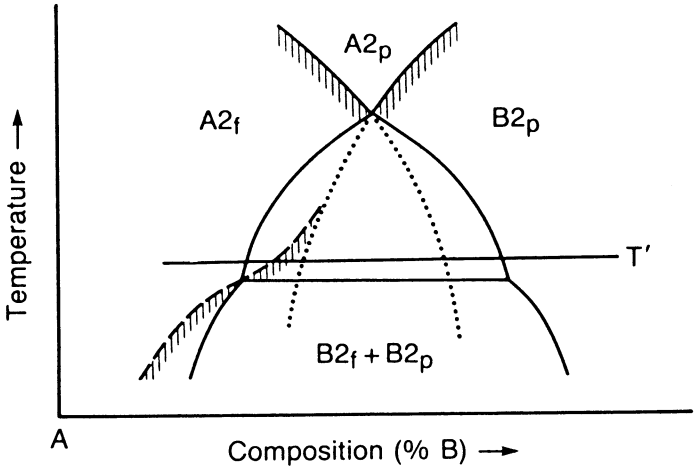

Figure 36a. Bicritical configuration and emergence of the stable doubly ordered phase at low temperature.

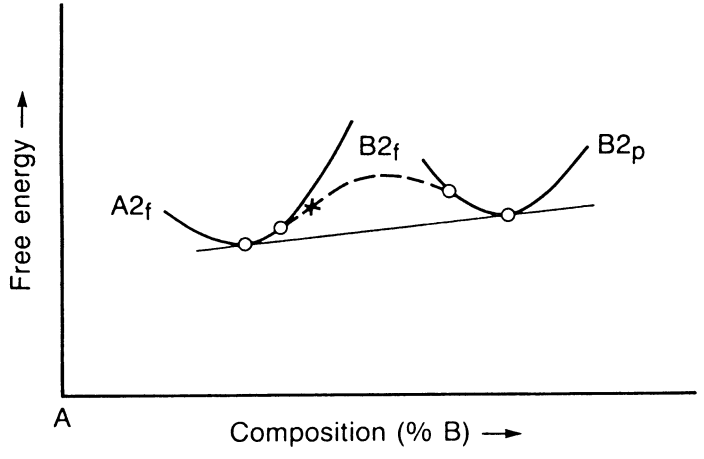

Figure 36b. Free energy *versus* composition diagram corresponding to T = T'. The doubly ordered phase is metastable over a small composition range and exhibits a spinodal point (x) and a limit of metastability.

point and several intersections of higher order transitions and first order boundaries is the Fe-Al binary shown schematically in Figure 37 (Semenovskaya, 1974). The system exhibits several atomically and magnetically ordered phases with corresponding critical end points and appropriate isotherms delineating the boundaries between the various two-phase fields. In such a system continuous phase separation or spinodal decomposition in different regions of temperature and composition is intimately related to the ordering tendencies which prevail. Furthermore, concomitant ordering and clustering phenomena have been revealed experimentally (Allen and Cahn, 1976; Allen, 1977).

5.3 Tetracritical Point

A *tetracritical point* is a special configuration where a "doubly ordered" phase becomes stable and four phases become indistinguishable, having the same free energy. A simple example of such a phase diagram in a binary system is shown in Figure 38a.

The four phases to be distinguished are:

$A2_p$ paramagnetic disordered bcc solid solution

$A2_f$ ferromagnetic, spin-ordered bcc solid solution

$B2_p$ atomically ordered CsCl-type paramagnetic phase

$B2_f$ ferromagnetic, atomically ordered solid solution

Below the *tetracritical* temperature the free energy *versus* composition diagram looks essentially as shown in Figure 38b. At the *tetracritical* temperature the free energy *versus* composition scheme is expected to look like Figure 39, where the free energies of the ordered and disordered phases are identical at a fixed composition. The extensions of the ordering transitions $A2_p \rightarrow A2_f$ and $A2_p \rightarrow B2_p$ may project into the doubly ordered single phase region (Figure 38a) or outside this region; see Figure 40. These two possibilities have been treated quantitatively in Landau formulation by Allen and Cahn (1982).

The Fe-Si system depicted in Figure 41 shows a composite of several of the critical points discussed above, including a *tetracritical* point. The complex ordering and clustering behavior of such a system can be interpreted simply along the lines developed in this overview. Without a systematic understanding of the individual multicritical behavior and convergence of first

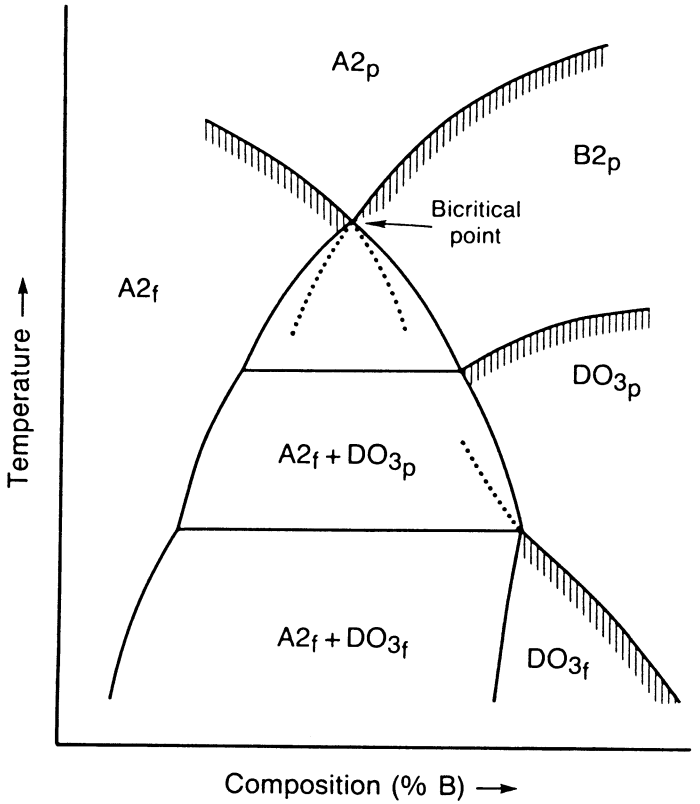

Figure 37. Schematic of the Fe-Al phase diagram exhibiting a bicritical point and higher order transition lines.

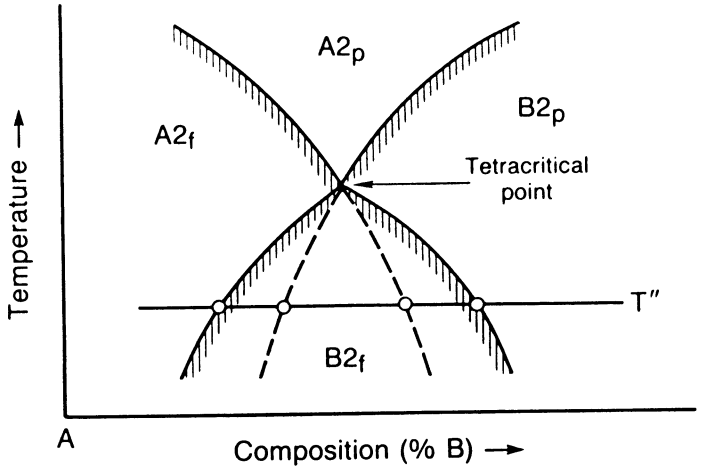

Figure 38a. A schematic of a phase diagram exhibiting a tetracritical point.

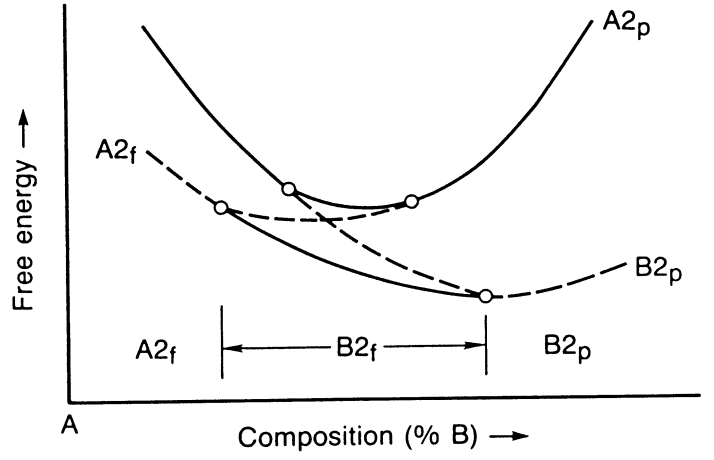

Figure 38b. Free energy *versus* composition curves at T = T″.

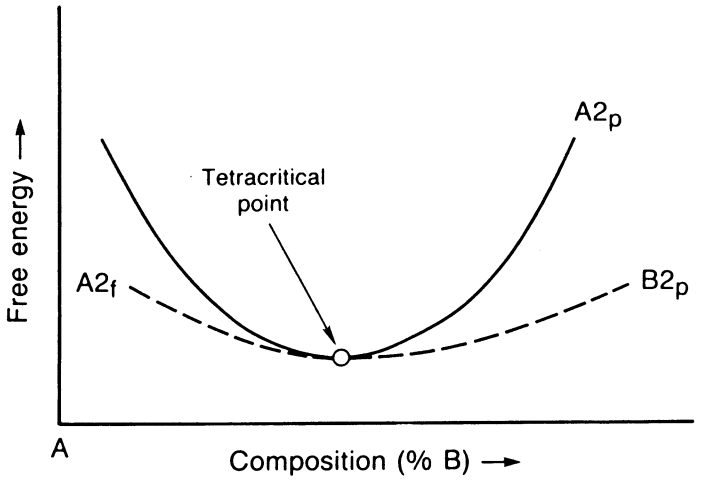

Figure 39. Free energy *versus* composition curves at the tetracritical temperature.

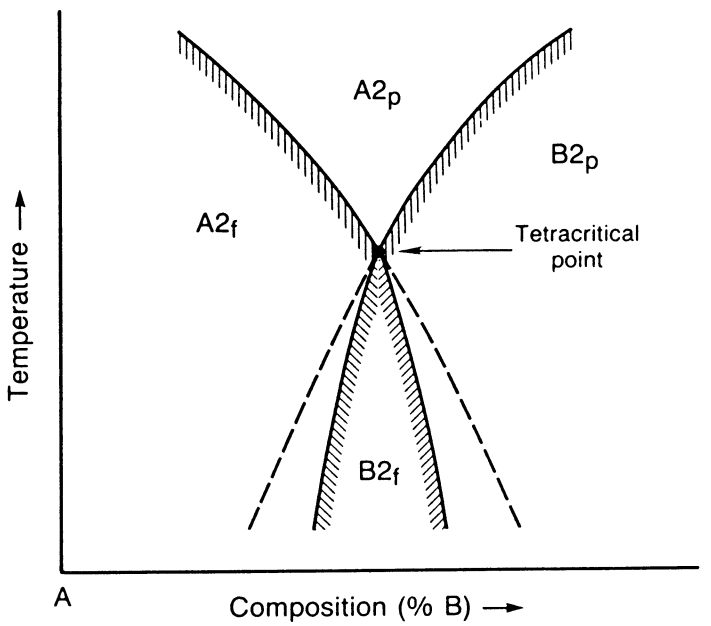

Figure 40. Schematic of a phase diagram of a tetracritical point showing an alternative projection of the lines of higher order transition.

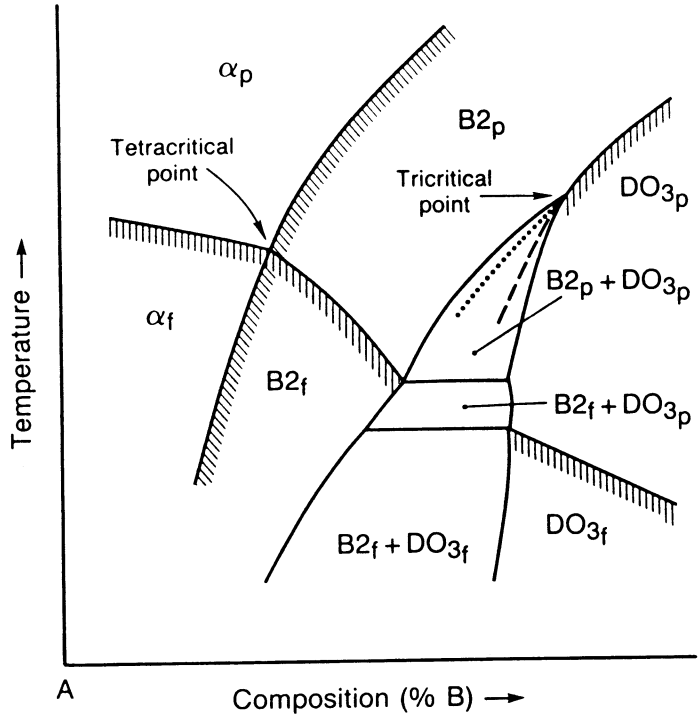

Figure 41. A schematic of the Fe-Si binary diagram exhibiting multicritical points.

order and higher order transitions, the sequences of ordering and phase separation in such a system would appear hopelessly complex.

6. CLOSURE

We have shown that the complex multistage reaction paths exhibited by solid solutions during their approach to equilibrium can be understood largely in terms of the thermodynamic stability of their initial states. The stability of a single phase state is determined by the behavior of the free energy as a function of the relevant order parameters. Continuous transformation of the initial state to a state of lower free energy derives from various thermodynamic instabilities which can be deduced from the phase diagram and its corresponding free energy curves. The simple geometric or graphical thermodynamic approach discussed herein is independent of particular solution models but reveals the essential features of the possible transformation behavior and phase equilibria. In this paper the interplay of atomic ordering, magnetic ordering and exsolution/clustering has been used to illustrate a range of phase transformation behavior that can be understood and systematized using this simple and essentially qualitative approach. Finally, an understanding of the full range of behavior exhibited by real systems with different ordering tendencies is only possible if lines of higher order transition and instability are appropriately included in the phase diagram, along with the usual first order phase boundaries.

ACKNOWLEDGEMENTS

The financial support from the National Science Foundation, Grants DMR-8413115 at Carnegie Mellon University and DMR-8611807 at the University of Pittsburgh is gratefully acknowledged.

REFERENCES

Aaronson, H.I. and K.C. Russell, in *Proceedings of International Conference on Solid→Solid Phase Transformations*, ed. by H.I. Aaronson, D.E. Laughlin, R.F. Sekerka and C.M. Wayman, Warrendale, PA, 371 (1982).

Allen, S.M. and J.W. Cahn, *Acta Met.* **24**, 425 (1976).

Allen, S.M., *Phil. Mag.* **36**, 181 (1977).

Allen, S.M. and J.W. Cahn, *Bulletin of Alloy Phase Diagrams*, **3**(3), 287 (1982).

Binder, K., C. Billotet and P. Mirold, *Z. Physik*, **B 30**, 183 (1978).

Buerger, M.J., *J. Chem. Phys.*, **15**, 1 (1947).

Cahn, J.W. and J.E. Hilliard, *J. Chem. Phys.* **28**, 258 (1958).

Cahn, J.W. and J.E. Hilliard, *J. Chem. Phys.* **31**, 688 (1959).

Cahn, J.W., *Acta Met.* **9**, 795 (1961).

Cahn, J.W., *Acta Met.* **10**, 179 (1962a).

Cahn, J.W., *Acta Met.* **10**, 907 (1962b).

Cahn, J.W. and R.J. Charles, *Phys. Chem. Glasses*, **6**, 181 (1965).

Cahn, J.W., *J. Chem. Phys.*, **42**, 93 (1965).

Cahn, J.W., *Trans. TMS-AIME*, **242**, 166 (1968).

Chou, A., A. Datta, G.H. Meier and W.A. Soffa, *J. Mat. Sci.*, **13**, 541 (1978).

Christian, J.W., *The Theory of Transformations in Metals and Alloys*, Pergamon Press, Oxford (1975).

Datta, A. and W.A. Soffa, *Acta Met.*, **24**, 987 (1976).

de Fontaine, D., *Solid State Physics*, **34**, 73 (1979).

de Fontaine, D., *Trans. of Met. Soc. AIME*, **245**, 1703 (1969).

de Fontaine, D. in *Ultrafine-Grain Metals*, ed. J.J. Burke and V. Weiss, Syracuse U. Press, Syracuse, N.Y., 93 (1970).

de Fontaine, D., *Acta Met.*, **23**, 553 (1975).

Gayle, F.W. and J.B. Vander Sande, *Bulletin of Alloy Phase Diagrams*, **5**(1), 19 (1984).

Griffiths, R.B., *Phys. Rev. Lett.*, **24**, 715 (1970).

Griffiths, R.B., *J. Chem. Phys.*, **60**, 195 (1974).

Hillert, M., Sc.D. Thesis, Massachusetts Institute of Technology (1956).

Hilliard, J., in *Phase Transformations*, ASM, 497 (1970).

Inden, G., *Bulletin of Alloy Phase Diagrams*, **2**(4), 412 (1982).

Ino, H., *Acta Met.* **26**, 827 (1978).

Khachaturyan, A.G., *Progress in Mat. Sci.*, **22**, 1 (1978).

Khachaturyan, A.G., *Theory of Structural Transformations In Solids*, John Wiley and Sons (1983).

Khachaturyan, A.G., T.F. Lindsey and J.W. Morris, *Met. Trans.* in press (1987).

Kubo, H. and C.M. Wayman, *Acta Met.*, **80**, 395 (1980).

Kulkarni, U.D., S. Banerjee and R. Krishnan, *Materials Science Forum* **3**, 111 (1985).

Langer, J.S., in *Fluctuations, Instabilities and Phase Transitions*, ed. by T. Riste, p. **19**, Plenum Press, N.Y. (1975).

Lin, J-C. and Y.A. Chang, *Met. Trans.*, in press (1988).

Martin, G., in *Solid State Phase Transformations in Metals and Alloys, Les Editions de Physique*, Orsay, France, 337 (1979).

Meijering, J.L., *Philips Res. Reports*, **18**, 138 (1963).

Miodownik, A.P., *Bulletin of Alloy Phase Diagrams* **2**(4), 406 (1982).

Nishizawa, T., M. Hasebe and M. Ko, *Acta Met.* **27**, 817 (1979).

Reuter, K.B., Ph.D. Thesis, Lehigh University (1987).

Semenovskaya, S.V., *Phys. Status Solidi*, **64**(b), 627 (1974).

Soffa, W.A. and D.E. Laughlin, in *Proceedings of an International Conference on Solid→Solid Phase Transformations*, ed. by H.I. Aaronson, D.E. Laughlin, R.F. Sekerka and C.M. Wayman, Warrendale, PA, 159 (1982).

Tiapkin, Y.D., *Ann. Rev. Mater. Sci.* **7**, 209 (1977).

such a solid solution passes through in order to attain thermodynamic equilibrium involves a knowledge of the phase diagram, the symmetry of the phases α and β, interphase interfacial free energies, as well as kinetic parameters such as diffusivity, *etc.* In this article we discuss several types of exsolution reactions that commonly occur in metallic or nonmetallic solid solutions.

We begin with the simplest exsolution reaction, namely one in which both the α and β phases have the same crystal structure, differing only in their respective compositions (2.1). This *isostructural* reaction can be modeled by only one "order parameter", namely the difference in composition between the two ensuing phases. The equilibrium value of this order parameter changes discontinuously at all points along the phase boundary (except at the critical point) and hence these transformations are thermodynamically classified as *first order*. We consider such exsolution reactions at both small supersaturations (2.2) and large supersaturations (2.3), namely under conditions in which the reaction may be modeled as nucleation or spinodal decomposition, respectively. We also discuss the case in which the supersaturation is of intermediate value, *viz.* the reaction occurs near the spinodal. In the discussion of spinodal decomposition, we differentiate between the microstructure of the reaction occurring in isotropic elastic media and that occurring in an anisotropic (cubic) elastic medium.

Another simple solid state reaction occurs when the parent α phase transforms entirely into an atomically ordered phase β, which is a crystallographic derivative (Buerger, 1947) of the α phase (3.1). In this case the reaction can be described by the long range (atomic) order parameter η. Such ordering reactions may be thermodynamically of either *first order* (3.2.2) or *higher order*[**] (3.2.1).

When a line of higher order transitions ends on a first order phase boundary, a *critical end* point exists (Allen and Cahn, 1982). If such a line terminates uniquely at the critical point of a two phase region, a *tricritical* point is produced at which three phases become indistinguishable (Griffiths, 1970 and 1974). Phase diagrams exhibiting *tricritical points* are herein presented, and the various possible reaction paths that exist for solid solutions exhibiting *tricritical* behavior are discussed (3.2.1).

The final sections (4 and 5) introduce another ordering reaction, namely "magnetic ordering". This entails an additional order parameter (M,

---

[**] We prefer to use the term "higher order" because of the difficulty in distinguishing between "second", "third", etc. order transitions. All "higher order" transitions are continuous at the transition temperature.